

Synthetic Antibiotic Derived from Sequences Encrypted in a Protein from Human Plasma

Angela Cesaro, Marcelo D. T. Torres, Rosa Gaglione, Eliana Dell'Olmo, Rocco Di Girolamo, Andrea Bosso, Elio Pizzo, Henk P. Haagsman, Edwin J. A. Veldhuizen, Cesar de la Fuente-Nunez,* and Angela Arciello*



Cite This: *ACS Nano* 2022, 16, 1880–1895



Read Online

ACCESS |



Metrics & More



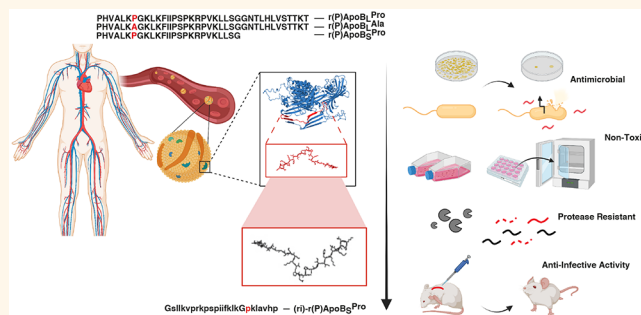
Article Recommendations



Supporting Information

ABSTRACT: Encrypted peptides have been recently found in the human proteome and represent a potential class of antibiotics. Here we report three peptides derived from the human apolipoprotein B (residues 887–922) that exhibited potent antimicrobial activity against drug-resistant *Klebsiella pneumoniae*, *Acinetobacter baumannii*, and *Staphylococci* both *in vitro* and in an animal model. The peptides had excellent cytotoxicity profiles, targeted bacteria by depolarizing and permeabilizing their cytoplasmic membrane, inhibited biofilms, and displayed anti-inflammatory properties. Importantly, the peptides, when used in combination, potentiated the activity of conventional antibiotics against bacteria and did not select for bacterial resistance. To ensure translatability of these molecules, a protease resistant retro-inverso variant of the lead encrypted peptide was synthesized and demonstrated anti-infective activity in a preclinical mouse model. Our results provide a link between human plasma and innate immunity and point to the blood as a source of much-needed antimicrobials.

KEYWORDS: encrypted peptides, human apolipoprotein B, antibiotic resistance, drug discovery, retro-inverso peptide design, anti-infective activity, nanopeptides



INTRODUCTION

In 2019 alone, more than 2.8 million people suffered from antibiotic-resistant infections and over 35 000 individuals died in the U.S.^{1,2} The ESKAPE pathogens (*Enterococcus faecium*, *Staphylococcus aureus*, *Klebsiella pneumoniae*, *Acinetobacter baumannii*, *Pseudomonas aeruginosa*, and *Enterobacter* species) are of particular concern as they are resistant to many available antibiotics.³ Indeed, it has been estimated that at the current rate of antibiotic resistance development 10 million people will die annually from untreatable infections by the year 2050. The World Health Organization has described this global problem as one of the biggest threats to human health.⁴

Therefore, alternatives to conventional antibiotics are urgently needed to treat such drug-resistant infections. We recently developed and used a computational tool able to search for encrypted peptides with antibiotic properties by systematically exploring the human proteome, an effort that yielded thousands of previously unexplored molecules.^{5–7} These precursor proteins, not necessarily related to host innate immune defense, contain within their sequence encrypted peptides that may be released upon proteolytic cleavage by bacterial or host proteases.^{7,8} Once they have carried out their

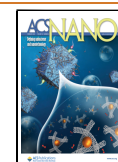
physiological function, numerous human proteins represent potential precursors of peptides with unrelated biological activity, including antimicrobial peptides.⁹ Thus, the presence of these peptide fragments, hidden within proteins, may reflect an evolutionary mechanism to increase the range of functionalities of proteins.¹⁰ Collectively, human encrypted peptides represent a previously untapped class of potential antibiotics.^{10,11}

Here, we describe encrypted peptides derived from the plasma protein human apolipoprotein B.¹² Plasma lipoproteins, such as high-density, low-density, and very low-density lipoproteins (HDL, LDL, and VLDL), play a key role in lipid transport among tissues and organs.^{6,13,14} Apolipoprotein B is responsible for carrying lipids, including cholesterol, around the body to cells within all tissues, and high levels of

Received: May 27, 2021

Accepted: December 27, 2021

Published: February 3, 2022



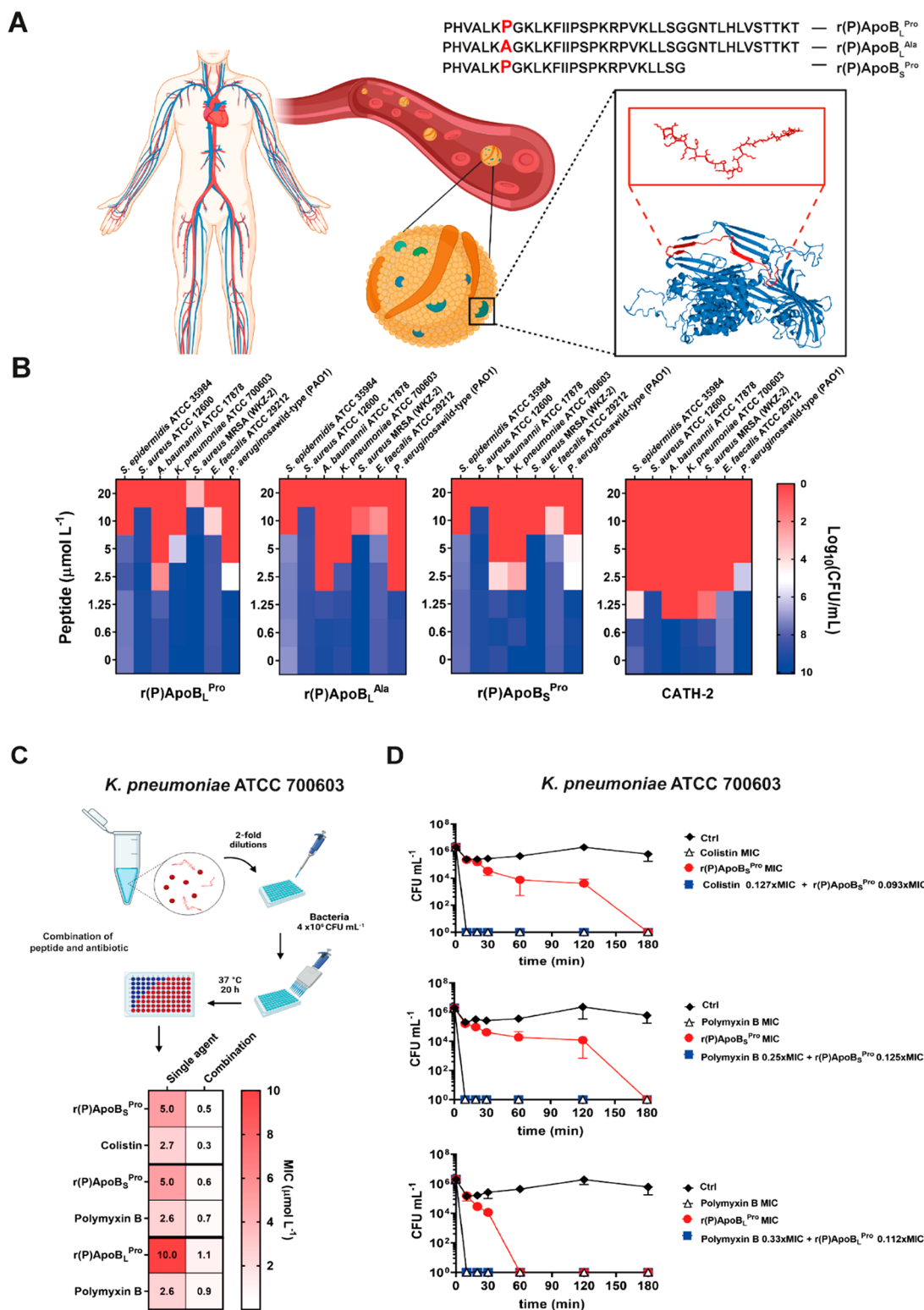


Figure 1. Antimicrobial activity and synergistic interactions of ApoB-derived encrypted peptides. (A) Schematic representation of the proteolytic release of ApoB-derived encrypted peptides from precursor human plasma apolipoprotein B, the main constituent of low-density lipoproteins; the sequences of each peptide are also reported. (B) Antimicrobial activity analyzed by testing peptide concentrations ranging from 0 to 20 $\mu\text{mol L}^{-1}$ (0–80 $\mu\text{g mL}^{-1}$ for peptide r(P)ApoB_L^{Pro} or r(P)ApoB_L^{Ala}, 0–40 $\mu\text{g mL}^{-1}$ for peptide r(P)ApoB_S^{Pro}, and 0–75 $\mu\text{g mL}^{-1}$ for peptide CATH-2) of ApoB-derived encrypted peptides against seven bacterial strains; reported data refer to assays carried out in triplicate and heat maps show averaged log (CFU mL⁻¹) values. (C) Schematic representation of peptide, colistin and polymyxin B concentrations used in combinatorial therapy. (D) Killing kinetic curves obtained by treating *K. pneumoniae* ATCC 700603 with the lead combinations of ApoB-derived encrypted peptides and colistin or polymyxin B; curves have been compared with those obtained by incubating cells with single agents at bactericidal concentrations. Groups treated with colistin MIC or polymyxin B MIC and colistin 0.127 ×

Figure 1. continued

MIC + r(P)ApoB_S^{Pro} 0.093 × MIC, polymyxin B 0.25 × MIC + r(P)ApoB_S^{Pro} 0.125 × MIC or polymyxin B 0.33 × MIC + r(P)ApoB_L^{Pro} 0.112 × MIC overlap in the figure.

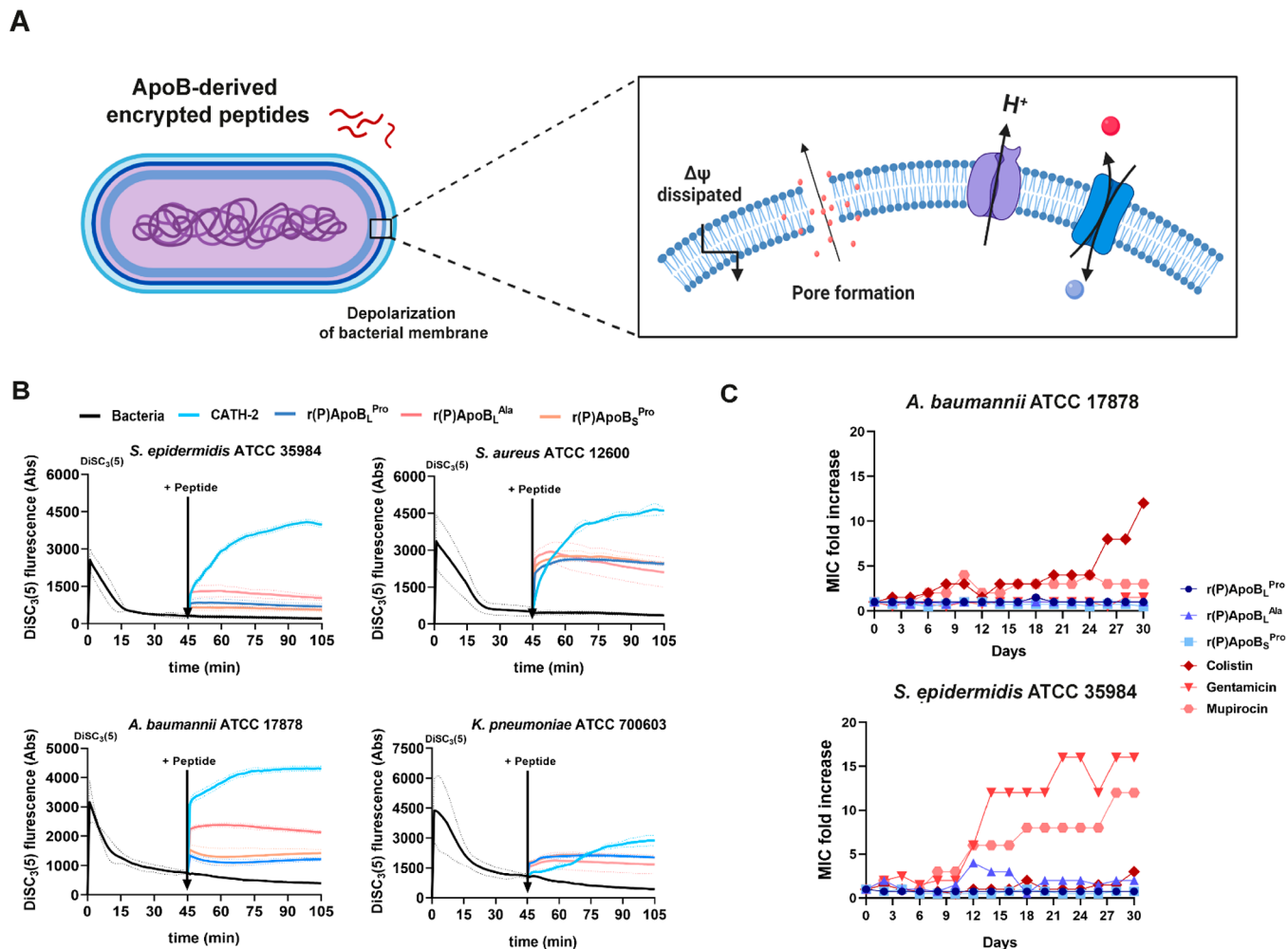


Figure 2. Mechanism of action and resistance development studies. (A) Schematic representation of ApoB-derived encrypted peptides effects on bacterial transmembrane potential ($\Delta\psi$). (B) Analysis of fluorescence intensity variation upon bacterial treatment with ApoB-derived encrypted peptides and CATH-2 peptide (positive control) in the presence of diSC₃(5) dye; the data refer to untreated control bacterial cells. Assays have been carried out in triplicate, and the data represent the mean \pm standard deviation. (C) Evaluation of resistance phenotype development upon prolonged treatment of *A. baumannii* ATCC 17878 and *S. epidermidis* ATCC 35984 with colistin, gentamicin, mupirocin, r(P)ApoB_L^{Pro}, r(P)ApoB_L^{Ala}, and r(P)ApoB_S^{Pro}. Assays were carried out in duplicate, and the data represent the mean fold change in MIC value over time.

apolipoprotein B are associated with heart disease.¹⁵ We provide experimental evidence that these encrypted peptides exhibit antimicrobial properties, target bacteria by depolarizing and permeabilizing their cytoplasmic membrane, display immunomodulatory activity and excellent cytotoxicity profiles, and potentiate the antimicrobial activity of conventional antibiotics. Importantly, these peptides do not select for bacterial resistance mechanisms, which traditionally hinder antibiotic efficacy. We characterized in detail their cytotoxicity profile and activity against drug-resistant bacteria both *in vitro* and in an animal model. Finally, we reprogram the lead compound into a protease-resistant retro-inverso synthetic variant composed entirely of D-amino acids and demonstrate its anti-infective potential in a preclinical mouse model. Collectively, these results provide a link between human

plasma and innate immunity and point to human blood as a previously untapped source of much-needed antimicrobials.

RESULTS AND DISCUSSION

Antimicrobial Properties of ApoB-Derived Encrypted Peptides. Numerous precursor proteins containing encrypted peptides with biological functions that are unrelated to those of the parent protein have been recently found throughout the human body, thus representing an alternative source for antibiotic discovery.^{7,10} Plasma lipoproteins or apolipoproteins, such as human apolipoprotein B (ApoB-100), are water-soluble complexes composed of lipids and one or more proteins.¹⁶ The concentration of ApoB in normal plasma is approximately 1.1 mg mL⁻¹.¹⁷ Plasma ApoB, in addition to its physiological role, seems to play an important role in bacterial

neutralization.¹⁸ Using an algorithmic approach selecting for physicochemical features as a scoring function,¹⁹ encrypted peptides within the sequence of human ApoB (amino acids 887–922) were identified. A promising antimicrobial region was identified according to the computational scores assigned to the amino acid sequences of two ApoB-100 isoforms. Next, we recombinantly produced in *Escherichia coli* three versions of the identified encrypted peptide, namely, r(P)ApoB_L^{Pro}, r(P)ApoB_S^{Pro}, and r(P)ApoB_L^{Ala}. These sequences present a Pro residue at the N-terminal extremity because of the acidic cleavage of an Asp–Pro bond necessary to excise peptides of interest from the rest of the recombinant construct.^{6,8,14,20} The ApoB peptide variants were labeled with Pro and Ala indicating their amino acid residue in position 7, which corresponds to the mutation differentiating the two isoforms. The labels L and S refer to a longer or a shorter version of the identified amino acid sequence and correspond to the relative and absolute scores, respectively, generated by the algorithm.⁶

First, we assessed the antimicrobial activity of ApoB-derived encrypted peptides against the following bacterial pathogens: *Staphylococcus epidermidis* ATCC 35984, *Staphylococcus aureus* ATCC 12600, *Acinetobacter baumannii* ATCC 17878, *Klebsiella pneumoniae* ATCC 700603, *Staphylococcus aureus* MRSA (WK7–2), *Enterococcus faecalis* ATCC 29212, and *Pseudomonas aeruginosa* wild-type (PAO1) using broth microdilution assays²¹ to determine their minimal inhibitory concentration (MIC) values, experimentally defined as the lowest antimicrobial concentrations that entirely inhibit bacterial growth. The peptides were found to exert significant antibacterial effects (MICs ranging from 2.5–20 $\mu\text{mol L}^{-1}$) against all the bacterial strains tested. *S. epidermidis* ATCC 35984, *S. aureus* ATCC 12600, *S. aureus* MRSA (WK7–2), and *E. faecalis* ATCC 29212 were found to be susceptible to the encrypted peptides at 10–20 $\mu\text{mol L}^{-1}$. The peptides were even more active against *A. baumannii* ATCC 17878, *K. pneumoniae* ATCC 700603, and *P. aeruginosa* wild-type (PAO1) with MIC values ranging from 2.5 to 5 $\mu\text{mol L}^{-1}$, thus indicating the increased ability of the peptides to target Gram-negative bacteria (Figures 1B and S1A, Table S1). The antimicrobial activities of these peptides (2.5–20 $\mu\text{mol L}^{-1}$) are similar to that of another peptide identified in human apolipoprotein E¹³ and other potent peptide antimicrobials such as TsAP-2, HM2 and HMS, ranalexin, and stylin 2.²²

To understand the antibacterial mechanism of action of ApoB-derived peptides, we evaluated their ability to depolarize bacterial membranes by using the voltage-sensitive dye diSC₃(5) in the presence of live bacterial cells, which is a cationic membrane-permeable fluorescent dye that penetrates lipid bilayers and accumulates in polarized cells.²³ The aggregation of diSC₃(5) molecules lead to a fluorescence quenching effect, lasting about 45 min in our experiments. Upon membrane depolarization, the dye molecules are rapidly released because of their cationic nature, leading to increased fluorescence intensity.²⁴ We used peptide CATH-2 as a positive control since it is known to exert antimicrobial activity by depolarizing the cytoplasmic membrane of bacteria.^{25,26} In our experiments, an increase in fluorescence intensity, indicating membrane depolarization, was observed in all pathogens tested when treated with ApoB-derived peptides in the presence of the voltage-sensitive dye diSC₃(5) (Figure 2A,B). To provide more insights into the mechanisms of action of ApoB-derived peptides, outer-membrane permeabilization assays were carried out using the Gram-negative bacteria *A.*

baumannii ATCC 17878 and *K. pneumoniae* ATCC 700603 (Figures S2). All peptides were found to permeabilize the outer membrane as indicated by an increase in the fluorescent signal associated with the lipophilic dye NPN. The fluorescent NPN probe produced a weak fluorescence in aqueous environments (control samples without peptides), but its fluorescence increased upon contact with the lipidic environment generated by bacterial membrane damage induced by peptide treatment (Figures S2). These data clearly reveal the ability of ApoB-derived peptides to damage and permeabilize the bacterial outer membrane of Gram-negative bacteria. Altogether, our data demonstrate that the peptides induced membrane depolarization and outer membrane permeabilization, thus leading to variations in the membrane potential, membrane damage, and eventual cell death, mechanisms that are shared with other peptides including several cathelicidins, melittin, and the ion channel-forming gramicidin D.^{27–31}

Next, we assessed the ability of the peptides to potentiate the antimicrobial activity of conventional antibiotics *via* synergistic interactions. Indeed, through synergistic or additive interactions, antimicrobial agents can significantly reduce their therapeutic dose, thus minimizing undesired side effects such as the selection of bacterial resistant phenotypes.^{32,33} To assess such interactions, we carried out checkerboard assays and determined the Fractional Inhibitory Concentration (FIC) index in each case.^{34–36} First, we determined the antimicrobial activity of each peptide when used as a monotherapy (Figure S1B and Table S2). Checkerboard assays revealed widespread additive effects ($0.5 > \text{FIC index} > 1$; light purple color in Figure S1C) when peptides were combined with conventional antimicrobials, such as vancomycin, erythromycin, gentamicin, clindamycin, and EDTA. Importantly, peptides r(P)ApoB_L^{Pro} and r(P)ApoB_S^{Pro} synergized with the LPS binders polymyxin B and colistin against the Gram-negative pathogen *K. pneumoniae* ATCC 700603 (Figure 1C; FIC index ≤ 0.5 ; purple signals in Figure S1C), thus significantly reducing both the peptide and antibiotic doses needed to eradicate this bacterium. Altogether, synergistic effects were detected when testing ApoB-derived encrypted peptides in combination with antibiotics that are active toward bacterial membranes (*e.g.*, polymyxin B and colistin), whereas additive interactions were observed when combined with antibiotics that inhibit protein synthesis (*e.g.*, erythromycin, clindamycin, and gentamicin) and target the bacterial cell wall (*e.g.*, vancomycin). The synergistic effects observed between the encrypted peptides and conventional antibiotics were further confirmed by changes in cell morphology observed in scanning electron microscopy (SEM) assays (Figure S1D). Combinations of r(P)ApoB_S^{Pro} ($0.093 \times \text{MIC} = 0.46 \mu\text{mol L}^{-1}$) and colistin ($0.127 \times \text{MIC} = 0.34 \mu\text{mol L}^{-1}$) altered the morphology of *K. pneumoniae* ATCC 700603 and substantially decreased bacterial viability (Figure S1D) at nonantimicrobial concentrations for each agent when tested alone (Figure S1D).

We also assessed the ability of ApoB encrypted peptides to potentiate each other's activity through synergistic interaction assays. Combinations of two or three peptides were investigated (Figure S4A,B). Indifferent interactions were obtained for combinations between two peptides (Figure S4A). Interestingly, combinations among three peptides led to decreased FIC values indicative of additive interactions (Figure S4B).

Longitudinal killing assays were carried out to evaluate the efficacy over time of the most promising combinations of

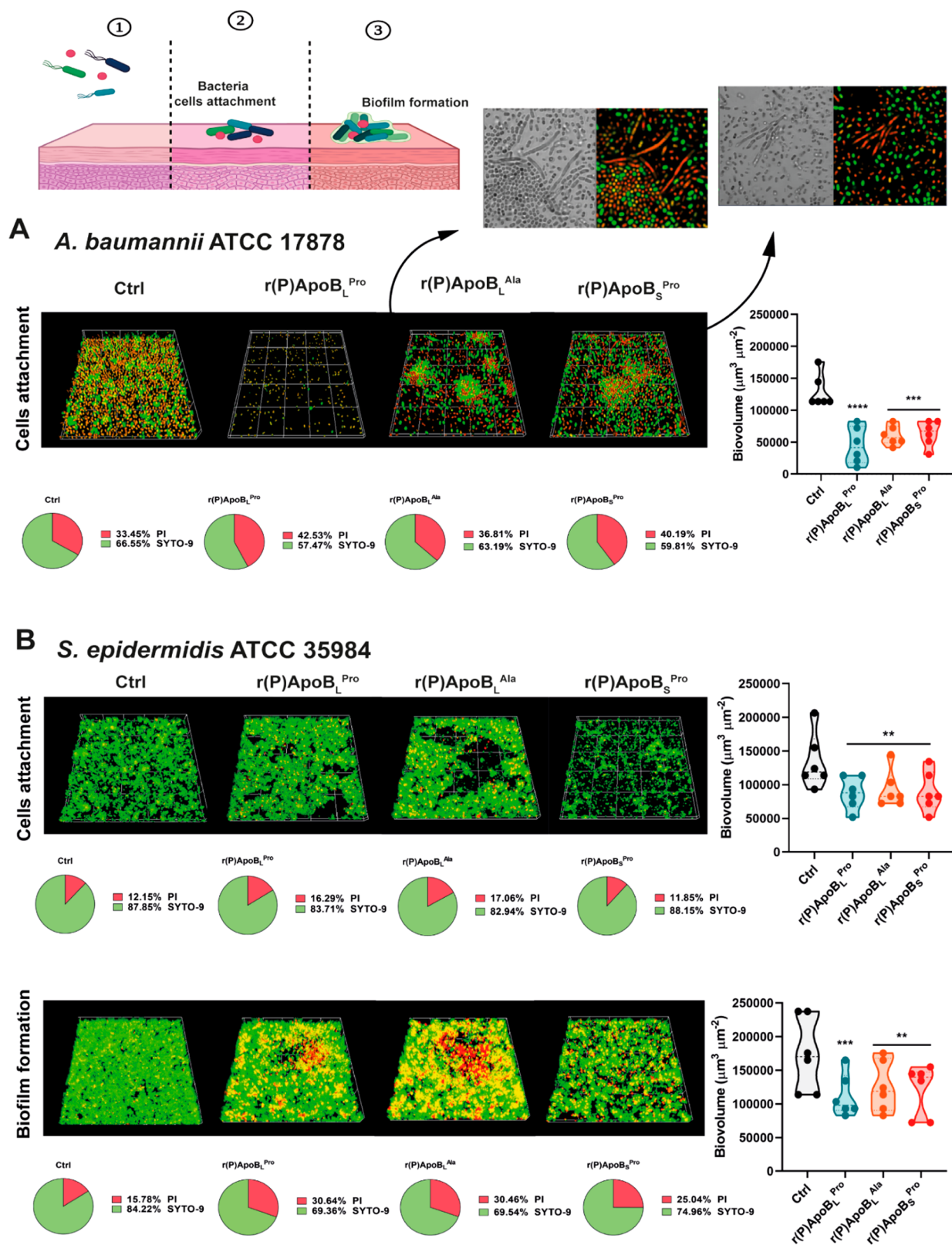


Figure 3. Antibiofilm activity of encrypted peptides derived from ApoB. Schematic representation of two stages of bacterial biofilm development. Effects of ApoB-derived encrypted peptides on cells attachment and biofilm formation in the case of (A) *A. baumannii* ATCC 17878 and (B) *S. epidermidis* ATCC 35984 by CLSM imaging. Significant differences for treated versus control samples were indicated as follows: *, $P < 0.05$; **, $P < 0.001$; or ***, $P < 0.0001$. Each experiment was carried out in triplicate.

antimicrobials. A longer exposure to antimicrobials is generally associated with an increased likelihood of selecting for bacterial resistance.³⁷ Kinetic killing curves were obtained by con-

comitantly treating bacteria with combinations of ApoB-derived encrypted peptides and colistin or polymyxin B. The speed of killing by antimicrobial peptides (AMPs) is usually

attributed to different mechanisms of action. Indeed, most AMPs present more than one mechanism of action, conferring an evolutionary advantage over the single mode of action of standard antibiotics.^{38,39} The two main reasons affecting killing kinetics are (i) membrane dysfunction following disruption of the phospholipid bilayer and/or (ii) interaction with intracellular targets involved in critical cellular processes, such as RNA and DNA replication and protein synthesis.⁴⁰ AMPs are generally potent and rapid bactericidal agents, causing significant bacterial death within 2 h.⁴¹ Consistent with this, peptides r(P)ApoB_L^{Pro} and its shorter derivative r(P)ApoB_S^{Pro} took 1 and 3 h, respectively, to completely kill bacterial cultures (Figure 1D). Again, significant antimicrobial effects were observed at concentrations much lower than those required when these agents were administered alone (Figure 1C,D). Moreover, combination therapy killed bacteria much more rapidly (within 10 min) than did monotherapy (60 or 180 min) (Figure 1D).

In addition, we carried out experiments to assess whether prolonged exposure to ApoB-derived encrypted peptides led to the evolution of resistant phenotypes, since classical AMPs are known to be less likely to trigger bacterial resistance than standard antibiotics.⁴² The Gram-negative bacterial pathogen *A. baumannii* ATCC 17878 and the Gram-positive pathogens *S. epidermidis* ATCC 35984 and *S. aureus* ATCC 12600 were longitudinally treated with r(P)ApoB_L^{Pro}, r(P)ApoB_L^{Ala}, and r(P)ApoB_S^{Pro}. Control sample groups were treated with the antibiotics colistin, gentamicin, and mupirocin, selected based on their distinct mechanisms of action: the former destabilizes the bacterial extracellular membrane, and the latter acts on intracellular targets. After 30 days of treatment, the MIC values of colistin and mupirocin increased against *A. baumannii* from 3.12 to 25 $\mu\text{g mL}^{-1}$ (2.7–21.6 $\mu\text{mol L}^{-1}$) and from 100 to 400 $\mu\text{g mL}^{-1}$ (200–800 $\mu\text{mol L}^{-1}$), respectively. The MIC values of gentamicin and ApoB-derived encrypted peptides did not change under the experimental conditions tested over the period of the experiment, indicating that *A. baumannii* did not develop resistance against either gentamicin or the encrypted peptides. Conversely, when *S. epidermidis* cells were exposed to gentamicin and mupirocin, MIC values increased from 3.12 to 50 $\mu\text{g mL}^{-1}$ (16.5–104.7 $\mu\text{mol L}^{-1}$) and from 0.0015 to 0.012 $\mu\text{g mL}^{-1}$ (0.003–0.024 $\mu\text{mol L}^{-1}$). No significant resistance development was observed for *S. epidermidis* when treated with ApoB-derived encrypted peptides or colistin (Figure 2C). *A. baumannii* resistance toward colistin increased by up to 8-fold, whereas *S. epidermidis* resistance to gentamicin and mupirocin increased by up to 16- and 8-fold, respectively (Figure 2C). Moreover, when we treated *S. aureus* ATCC 12600 with each peptide or the selected antibiotics, no variations in the MIC values were observed (Figure S3) except for mupirocin, whose MIC value increased 8-fold from 0.024 to 0.19 $\mu\text{g mL}^{-1}$ (0.048–0.38 $\mu\text{mol L}^{-1}$) between days 15 and 21 of treatment (Figure S3). Importantly, *A. baumannii*, *S. epidermidis*, and *S. aureus* ATCC 12600 did not develop resistance to the encrypted peptides under our experimental conditions (Figures 2C and S3), thus underlining their promise as antimicrobials that do not readily select for bacterial resistance. SEM results also revealed that the strains that evolved resistance displayed different morphologies than their antibiotic-susceptible predecessors. For example, both colistin-resistant *A. baumannii* ATCC 17878 and gentamicin-resistant *S. epidermidis* ATCC 35984 presented wrinkled borders (Figure S1E) as opposed to

the smooth colonies' characteristic of their morphology at the beginning of the experiment (Figure S1E).

Antibiofilm Effects of ApoB-Derived Encrypted Peptides. We carried out crystal violet assays to investigate whether ApoB-derived encrypted peptides prevented biofilm formation of common skin bacterial pathogens, such as *S. epidermidis* ATCC 35984, *S. aureus* ATCC 12600, *A. baumannii* ATCC 17878, and *K. pneumoniae* ATCC 700603. The effects of the peptides on the three main stages of biofilm development (*i.e.*, adhesion, formation, and preformed biofilm)⁴³ were analyzed using the crystal violet assay.⁴⁴ Sub-MIC peptide concentrations ranging from 1.25 to 5 $\mu\text{mol L}^{-1}$ led to significant inhibition (30–40%) of biofilm adhesion and formation in the Gram-negative strains *A. baumannii* ATCC 17878 and *K. pneumoniae* ATCC 700603 and in the Gram-positive bacterium *S. epidermidis* ATCC 35984. Conversely, no significant effects were detected on biofilm adhesion and formation of *S. aureus* ATCC 12600 or preformed biofilms of any of the pathogens tested (Figure S5). We also carried out confocal laser scanning microscopy (CLSM) experiments to assess the effects of each peptide against *A. baumannii* ATCC 17878 and *S. epidermidis* ATCC 35984. The peptides significantly altered biofilm architecture and reduced biofilm biovolume in both strains. Peptide r(P)ApoB_L^{Pro} was found to exert the strongest effect (biovolume reduced by 3-fold compared to the untreated control) against *A. baumannii* ATCC 17878 initial biofilm attachment, whereas r(P)ApoB_L^{Ala} and r(P)ApoB_S^{Pro} triggered cell filamentation in *A. baumannii*, suggesting that they may interfere with cell division mechanisms by blocking septation,¹⁴ consistent with the high percentage of dead cells observed (Figure 3A). No significant effects for any of the peptides were observed on *A. baumannii* biofilm formation (Figure S6). However, the three ApoB-derived peptides affected the biofilm matrix and reduced the biofilm biovolume of *S. epidermidis* ATCC 35984 at sub-MIC concentrations (5 $\mu\text{mol mL}^{-1}$). Peptides r(P)ApoB_L^{Pro} and r(P)ApoB_L^{Ala} further affected biofilm formation by inducing cell death (*i.e.*, red cell aggregates in Figure 3B). Overall, our data suggest that ApoB-derived encrypted peptides exert their antibiofilm activity against *S. epidermidis* ATCC 35984 through multiple mechanisms (Figure 3B). The antibiofilm activity of these molecules is comparable to that of human hepcidin 20, an AMP secreted by hepatocytes that at concentrations ranging from 3.15 to 25 $\mu\text{mol L}^{-1}$ reduces the extracellular matrix mass, alters biofilm architecture, and targets polysaccharide intercellular adhesin in *S. epidermidis*.⁴⁵

Biocompatibility and Anti-Inflammatory Effects of Encrypted Peptides. Cytokine-mediated immunogenicity is one potential side effect of peptide therapeutics as it can lead to cytotoxic effects and allergic responses.^{22,46} To determine whether the peptides exerted any toxic effects against eukaryotic cells and to verify their biocompatibility toward skin cell cultures, we carried out dose–response and time-course 3-(4, 5-dimethylthiazolyl-2)-2,5-diphenyltetrazolium bromide (MTT) and lactate dehydrogenase (LDH) cytotoxicity assays against both human dermal fibroblasts (HDF) and human epidermoid carcinoma cell (A431) lines. Due to their cationic nature, most AMPs preferentially interact with negatively charged membranes, such as those of bacteria. The presence of cholesterol and the absence of acidic phospholipids in normal human cell membranes are at the basis of AMPs' selective toxicity toward prokaryotic cells.⁴⁷ Conversely, the net negative charge of tumoral cell

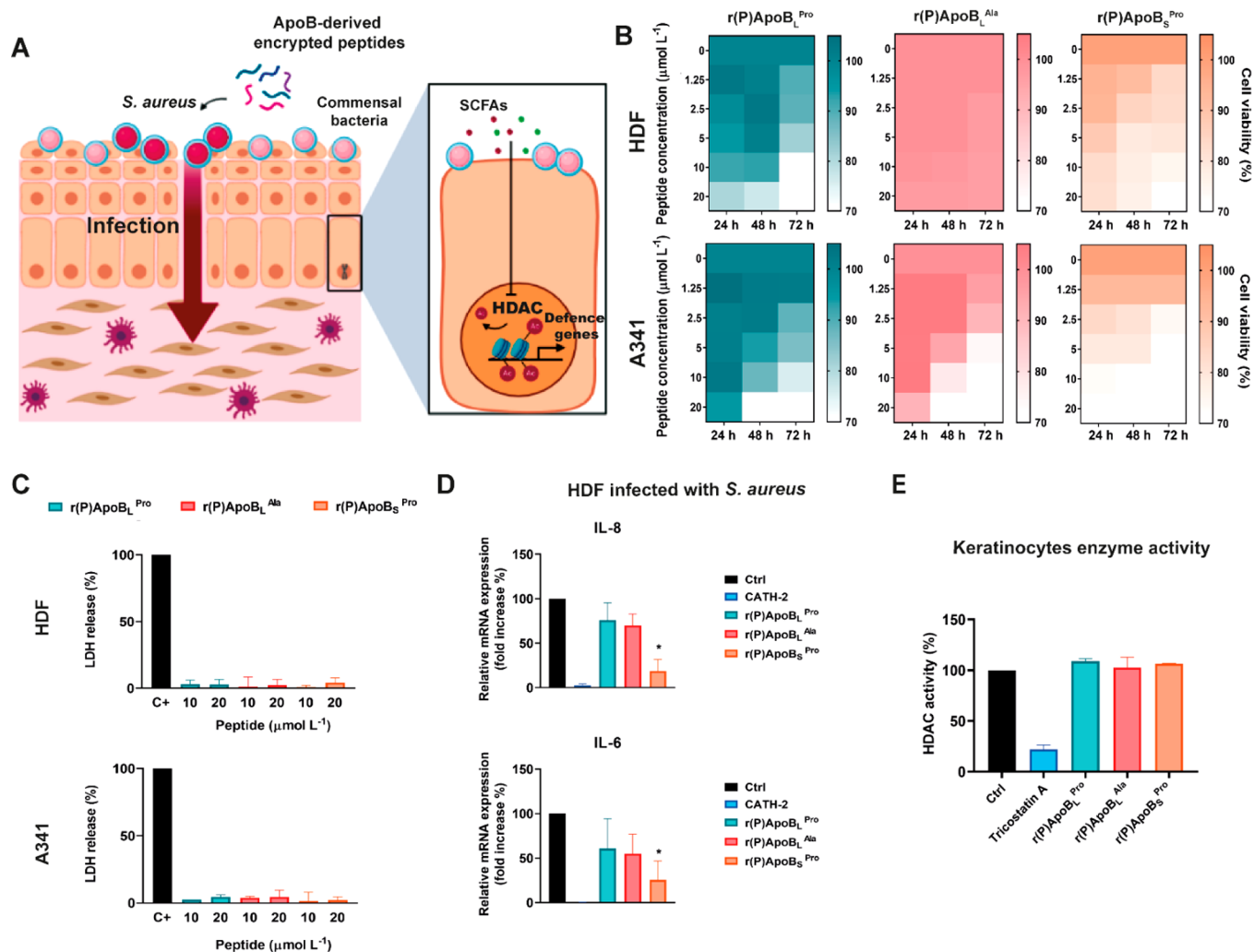


Figure 4. Biocompatibility and anti-inflammatory properties of ApoB-derived encrypted peptides. (A) Schematic representation of the skin barrier. (B) Cytotoxic effects of increasing concentrations of r(P)ApoB_L^{Pro} (blue), r(P)ApoB_L^{Ala} (pink), and r(P)ApoB_S^{Pro} (orange) on HDF (human dermal fibroblasts) and A431 (human epidermoid carcinoma cells) cell lines over time. (C) LDH release upon treatment of HDF and A431 cells with ApoB-derived encrypted peptides. The positive control was obtained by treating cells with lysis buffer. (D) ApoB-derived encrypted peptides effects on IL-8 and IL-6 expression in HDF cells infected with *S. aureus* ATCC 12600 analyzed by RT-qPCR. (E) Effects of ApoB-derived encrypted peptides on HDAC activity in HaCaT cells. HDAC activity is expressed as a percentage of the activity determined in untreated control cells. Significant differences for treated versus control samples are indicated as follows: *, $P < 0.05$.

membranes, conferred by modifications in phospholipid composition, promotes the anticancer activity of some AMPs.^{48–50} When incubated with normal human fibroblasts, ApoB-derived encrypted peptides exhibited mild toxicity (up to 20–30% decrease in cell viability) after 72 h of peptide treatment at 20 $\mu\text{mol L}^{-1}$. All peptides at 10–20 $\mu\text{mol L}^{-1}$ decreased carcinoma cell viability by 30–40% after 48–72 h (Figure 4B). r(P)ApoB_S^{Pro} reduced tumoral cell viability by 30% after 24 h (Figure 4B). To further analyze peptide biosafety toward normal and tumoral skin cells, we also tested the peptides at higher concentrations (25, 50, 100, and 200 $\mu\text{mol L}^{-1}$) (Figure S7). At 100 and 200 $\mu\text{mol L}^{-1}$, ApoB encrypted peptides decreased cell viability up to 30–40% of normal human fibroblasts and over 70% of human epidermoid carcinoma cells (Figure S7). These data confirm that the peptides are safe against normal cells at the doses required to exert antimicrobial properties. To evaluate whether peptides exert cytostatic or cytotoxic effects through membrane damage, LDH release in culture medium was detected as a biomarker of membrane damage.⁵¹ Thus, human dermal fibroblasts (HDF)

and human epidermoid carcinoma cells (A431) were treated with each peptide at a concentration of 10 and 20 $\mu\text{mol L}^{-1}$ for 72 h. No significant LDH release was detected, thus indicating no damage to eukaryotic cell membranes caused by exposure to the peptides (Figure 4C).

Enzyme-linked immunosorbent (ELISA) assays were also carried out to exclude any potential undesired inflammatory response triggered by treating human differentiated monocytes (THP-1) with the ApoB-derived encrypted peptides. We evaluated the levels of monocyte chemoattractant protein-1 (MCP-1), interleukin 8 (IL-8), and tumor necrosis factor (TNF α) in differentiated THP-1 cells upon treatment with each peptide at 5 or 20 $\mu\text{mol L}^{-1}$ for 24 h. No significant release of the pro-inflammatory cytokines IL-8 and TNF α or the chemokine MCP-1, which is involved in leukocyte activation and migration, was detected in peptide-treated groups compared to positive control samples incubated with 10 ng mL⁻¹ of lipopolysaccharide (LPS from *P. aeruginosa* PAO1) (Figure S11).¹³ Clinical studies have revealed that several skin diseases are associated with an increased

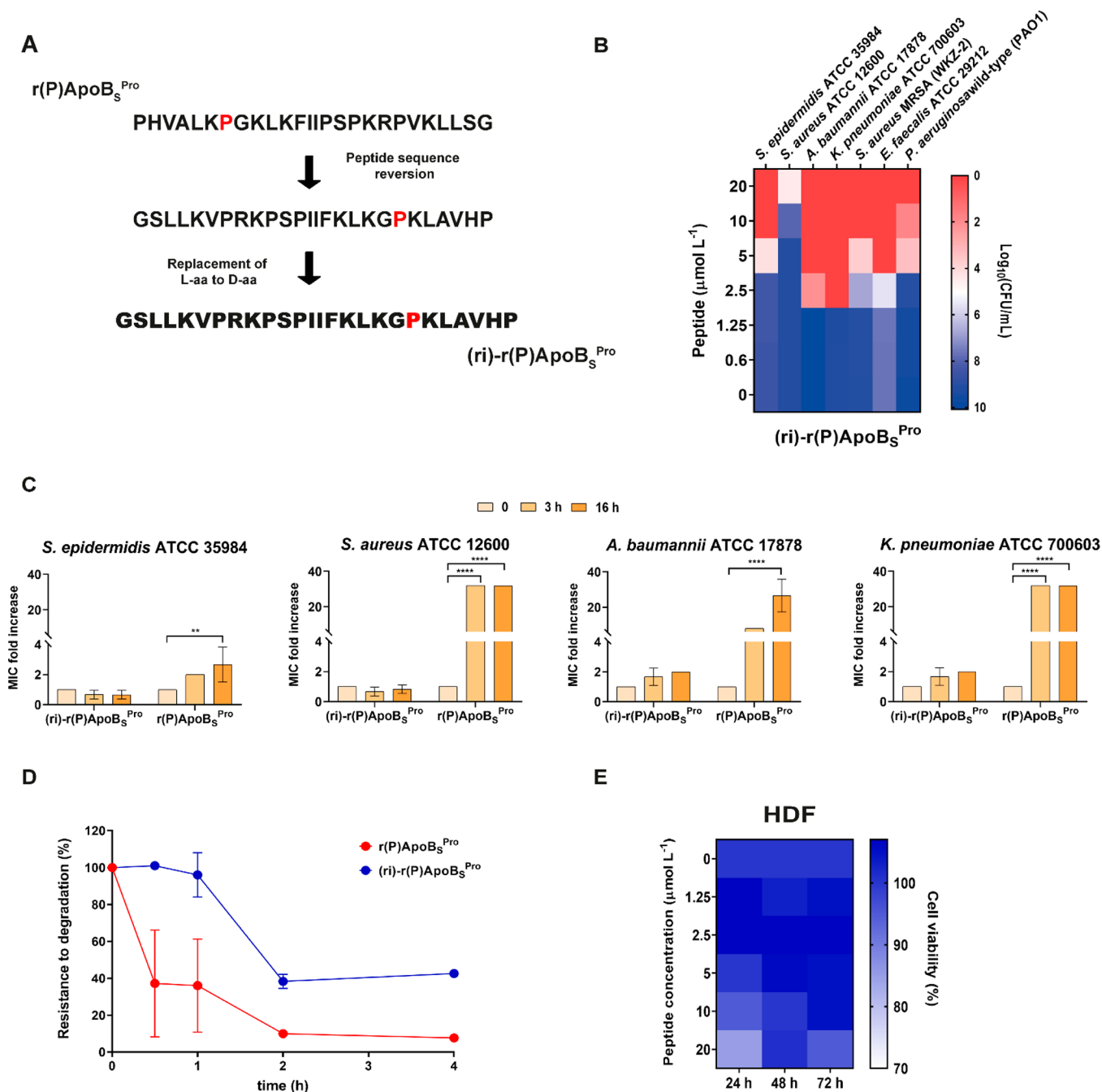


Figure 5. Stability, antimicrobial activity, and cytotoxic profile of retro-inverso synthetic peptide. (A) Schematic representation of retro-inverso peptide design leading to (ri)-r(P)ApoB_S^{Pro}. (B) Antimicrobial activity of (ri)-r(P)ApoB_S^{Pro} (μmol L⁻¹) against seven bacterial strains; reported data refer to assays carried out in triplicate and heat maps show averaged log (CFU mL⁻¹) values. (C) Antibacterial activity of (ri)-r(P)ApoB_S^{Pro} peptide against four bacterial strains after preincubation in 10% serum. Reported data refer to assays carried out in triplicate and the fold changes in antimicrobial activity are calculated as ratio between peptide MIC values obtained after and before incubation for 1 and 16 h in the presence of 10% serum at 37 °C. Statistical significance was determined using two-way ANOVA followed by Dunnett's test: *, $P < 0.01$, and ****, $P < 0.0001$. (D) Resistance to degradation of (ri)-r(P)ApoB_S^{Pro} exposed to fetal bovine serum (FBS) proteases for 4 h. (E) Cytotoxic effects of increasing concentrations of (ri)-r(P)ApoB_S^{Pro} on HDF (human dermal fibroblasts) cells. No significant differences were observed for the time points assessed.

inflammatory response induced by endogenous AMPs such as defensins and the cathelicidin LL-37, both of which trigger secretion of several cytokines at the injury site.⁵² ApoB-derived encrypted peptides operated differently, as they did not increase cytokine release.

Skin infections caused by opportunistic bacterial pathogens, such as *Staphylococci*, *Acinetobacter*, and *Pseudomonas* strains,

typically trigger the activation of a significant immune response in the underlying skin cells.⁵³ Recent studies demonstrated that *S. aureus* contributes to long-lasting cutaneous inflammation and local immunosuppression.⁵⁴ For this reason, we also evaluated the effects of ApoB-derived peptides on HDFs infected with *S. aureus* ATCC 12600, the primary pathogen infecting skin and soft tissues.⁵⁵ Using RT-qPCR, we assessed

the effects of ApoB-derived encrypted peptides ($10 \mu\text{mol L}^{-1}$) and the positive control peptide CATH-2 ($2.5 \mu\text{mol L}^{-1}$) on the expression of pro-inflammatory cytokines IL-8 and IL-6 (Figure 4D). Peptide $r(\text{P})\text{ApoB}_S^{\text{Pro}}$ reduced the inflammatory response triggered by HDFs infection with *S. aureus* ATCC 12600 (Figure 4D). It is worth noting that patients with psoriasis, a skin disorder associated with infections caused by *Streptococci* and *Staphylococcus* species, tend to have reduced ApoB plasma levels, thus indicating an interesting and complex role of this lipoprotein in host defense.⁵⁶ Our results (Figure 4D) are in line with prior studies describing the role of ApoB in controlling *S. aureus* virulence.⁵⁷ Conversely, no anti-inflammatory effects were observed (Figure S8) when we tested ApoB encrypted peptides (at 5 and $20 \mu\text{mol L}^{-1}$) in HDF cells infected with *A. baumannii* ATCC 17878. However, under the same conditions, $r(\text{P})\text{ApoB}_L^{\text{Ala}}$ and $r(\text{P})\text{ApoB}_S^{\text{Pro}}$ peptides (at 5 and $20 \mu\text{mol L}^{-1}$, respectively) were found to increase the expression levels of IL-8 and IL-6 (Figure S8). Stimulation of HDF with LPS from *E. coli* increased the expression levels of IL-8 and IL-6 compared to the expression levels in the same cells stimulated with LTA from *S. aureus* (Figure S9). When we tested ApoB encrypted peptides [$r(\text{P})\text{ApoB}_L^{\text{Pro}}$, $r(\text{P})\text{ApoB}_L^{\text{Ala}}$ and $r(\text{P})\text{ApoB}_S^{\text{Pro}}$] on HDF stimulated with LPS, they did not display any anti- or pro-inflammatory effects (Figure S10).

Histone deacetylase (HDAC) enzymes, encoded by the HDAC genes, play a key role in integrating commensal-bacteria-derived signals to calibrate epithelial cell responses.⁵⁸ Consequently, a decrease in HDAC activity in skin keratinocytes correlates with imbalances in physiological host–commensal interactions. Thus, to rule out any potential side effect of the peptides against skin cells, we assessed whether $r(\text{P})\text{ApoB}_L^{\text{Pro}}$, $r(\text{P})\text{ApoB}_L^{\text{Ala}}$, and $r(\text{P})\text{ApoB}_S^{\text{Pro}}$ affected the activity of HDAC enzymes. Briefly, HaCaT human keratinocytes were treated for 30 min with each peptide ($20 \mu\text{mol L}^{-1}$) and the selective HDAC inhibitor trichostatin A (50 nmol L^{-1}), which was used as a positive control. ApoB-derived encrypted peptides did not affect HDAC activity, indicating that they may not negatively influence the balance between skin microbiota and epithelial cells (Figure 4E).

In Vitro and In Vivo Antimicrobial Activity of Synthetic Retro-Inverso Peptide $r(\text{P})\text{ApoB}_S^{\text{Pro}}$. One of the main limitations hindering the development of peptide therapeutics is their low stability in complex biological environments that contain proteolytic enzymes.⁵⁹ Linear peptides are sensitive to proteolysis, drastically reducing their biological activity and their application as antimicrobial agents.⁶⁰ An approach to overcome proteolytic degradation of peptides involves the use of retro-inverso derivatives.⁵⁹ Simply replacing L-amino acids with D-amino acids, however, is generally ineffective as the side-chain orientation is completely altered with respect to the target.⁶¹ To guarantee structural stability, spatial orientation, side-chain topology, and overall peptide bioactivity, an alternative strategy is to engineer retro-derivatives, which can be built by reversing the D-peptide sequence while flipping its termini, thus restoring the L-amino side chain angles.^{35,61,62} Retro-inverso variants are known to present high topochemical similarities with their precursors and preserve bioactivities.

Peptide $r(\text{P})\text{ApoB}_S^{\text{Pro}}$ was selected as our lead compound derived from ApoB-100 because of its shorter length and excellent anti-infective and cytotoxic profiles (Figures 1B,C and 4B; Table S1). We proceeded to synthesize the retro-

inverso version of $r(\text{P})\text{ApoB}_S^{\text{Pro}}$ [*i.e.*, $(\text{ri})\text{-}r(\text{P})\text{ApoB}_S^{\text{Pro}}$] by reversing its peptide sequence and replacing all L-amino acids for their D-counterparts (Figure 5A). First, we evaluated the antimicrobial activity of $(\text{ri})\text{-}r(\text{P})\text{ApoB}_S^{\text{Pro}}$ against seven pathogens. Peptide $(\text{ri})\text{-}r(\text{P})\text{ApoB}_S^{\text{Pro}}$ displayed increased activity against Gram-negative rather than Gram-positive bacterial strains, as previously reported for its parent peptide $r(\text{P})\text{ApoB}_S^{\text{Pro}}$ (Figures 5B and S12; Table S3). The MIC values of $(\text{ri})\text{-}r(\text{P})\text{ApoB}_S^{\text{Pro}}$ ranged from 2.5 to $5 \mu\text{mol L}^{-1}$ against *A. baumannii* ATCC 17878, *K. pneumoniae* ATCC 700603, and *E. faecalis* ATCC 29212, whereas it was active at 10 and $20 \mu\text{mol L}^{-1}$ against *S. epidermidis* ATCC 35984, *S. aureus* ATCC 12600, *S. aureus* MRSA (WK7–2), and *P. aeruginosa* wild-type (PAO1), respectively, thus demonstrating that our synthesis modifications did not alter the antimicrobial profile of the original peptide.

To determine its proteolytic stability, we assessed whether $(\text{ri})\text{-}r(\text{P})\text{ApoB}_S^{\text{Pro}}$ was less susceptible to serum proteases compared to its parent peptide $r(\text{P})\text{ApoB}_S^{\text{Pro}}$. The MIC values of the peptide were measured upon incubation in 10% fetal bovine serum, which contains human endo- and exoproteases, for 1 and 16 h.⁶³ Whereas natural $r(\text{P})\text{ApoB}_S^{\text{Pro}}$ peptide completely lost its activity upon incubation in serum showing MIC values against *S. aureus* ATCC 12600, *A. baumannii* ATCC 17878, and *K. pneumoniae* ATCC 700603 of $>80 \mu\text{mol L}^{-1}$, as opposed to $5\text{--}20 \mu\text{mol L}^{-1}$ in regular medium (Figure 5C), the antimicrobial activity of $(\text{ri})\text{-}r(\text{P})\text{ApoB}_S^{\text{Pro}}$ retro-inverso peptide remained constant even after 16 h of preincubation in serum (Figure 5C). These antimicrobial activity results corroborate the degradation profile data obtained from analyzing aliquots of the peptide solution exposed to serum by using mass spectrometry coupled to liquid chromatography (Figure 5D). Indeed, the natural parent peptide degraded after 30 min of exposure to serum proteases, whereas $(\text{ri})\text{-}r(\text{P})\text{ApoB}_S^{\text{Pro}}$ demonstrated increased resistance by persisting ($\sim 50\%$ of initial concentration added) after 4 h of exposure to proteases in serum (Figure 5D). These results demonstrate the high stability of our engineered peptides when compared with previously described peptides in the literature.^{64–67} On the contrary, our other peptides composed of L-amino acids [*i.e.*, $r(\text{P})\text{ApoB}_L^{\text{Pro}}$, $r(\text{P})\text{ApoB}_L^{\text{Ala}}$, and $r(\text{P})\text{ApoB}_S^{\text{Pro}}$] were not stable in the presence of serum and degraded within minutes (Figure 5D), thus further underscoring the increased stability of our retro-inverso variant.

Additional experiments were carried out to verify the biocompatibility of $(\text{ri})\text{-}r(\text{P})\text{ApoB}_S^{\text{Pro}}$ toward skin cell cultures, since incorporating D-amino acids into peptide sequences may lead to toxic effects.⁶⁸ In the dose–response and time-course MTT cytotoxicity assays, peptide $(\text{ri})\text{-}r(\text{P})\text{ApoB}_S^{\text{Pro}}$ decreased human fibroblasts (HDFs) viability by 20–30% at the highest concentrations tested (100 and $200 \mu\text{mol L}^{-1}$) (Figures 5E and S13). Similar to $r(\text{P})\text{ApoB}_S^{\text{Pro}}$, the retro-inverso peptide displayed lower toxic effects toward HDFs than $r(\text{P})\text{ApoB}_L^{\text{Pro}}$ and $r(\text{P})\text{ApoB}_L^{\text{Ala}}$ (Figure 5E and S7). These data suggest that the shorter peptides [$r(\text{P})\text{ApoB}_S^{\text{Pro}}$ and $(\text{ri})\text{-}r(\text{P})\text{ApoB}_S^{\text{Pro}}$] present decreased toxicity compared to the longer peptide versions (Figures 4E, 5B, S7, and S13). Altogether, these results demonstrate that the substitution of L-amino acids by D-amino acids significantly increased peptide stability without altering its antimicrobial and cytotoxic activities, thus increasing the translational potential of this agent.

To assess the anti-infective potential of the peptides *in vivo*, we used a murine abscess infection model (Figure 6). The

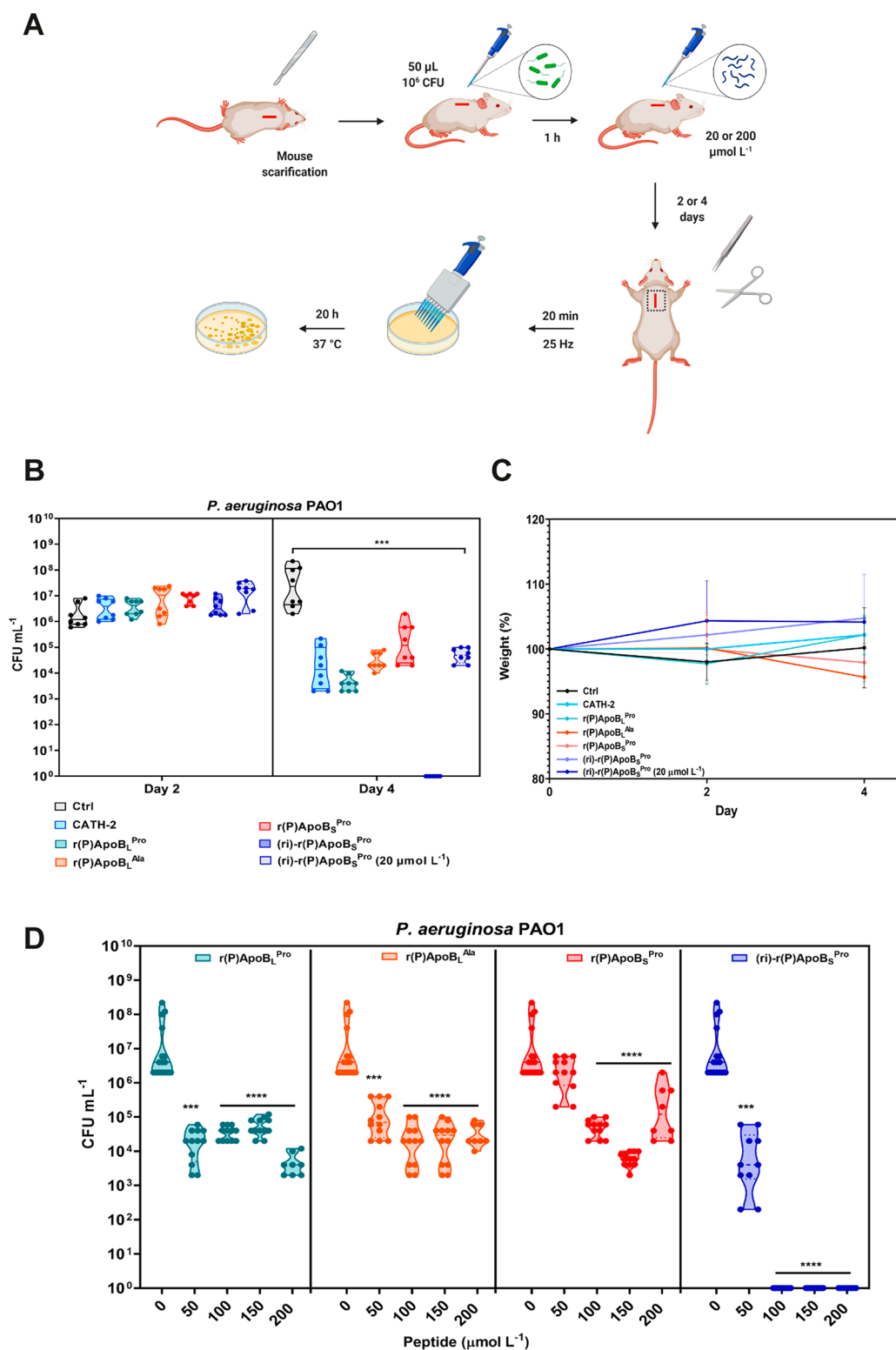


Figure 6. *In vivo* activity of natural and synthetic encrypted peptides derived from human ApoB. (A) Schematic representation of the *in vivo* experimental design. The back of each mouse was shaved, and an abrasion was generated to damage the stratum corneum and the upper layer of the epidermis. Subsequently, a 50 μL aliquot containing 10^6 CFU of *P. aeruginosa* PAO1 in PBS was inoculated over each defined area. At 1 h after the infection, peptides (20 or 200 $\mu\text{mol L}^{-1}$) were administered to the infected area. Four animals per group were euthanized at day 2 or 4 postinfection, and the area of scarified skin was excised and homogenized for 20 min (25 Hz). (B) Homogenized samples were serially diluted for CFU quantification. Statistical significance was determined using two-way ANOVA followed by Dunnett's test: ***, $P < 0.001$. (C) Mouse body weight measurements were carried out throughout the experiment and normalized by the body weight at the beginning of the experiment. (D) *In vivo* dose–response curves obtained by administering increasing concentrations of each peptide at the infection site at 1 h after the infection was established. Statistical significance was determined using two-way ANOVA followed by Dunnett's test: ***, $P < 0.001$.

Gram-negative bacterium *P. aeruginosa* PAO1, which is responsible for dangerous skin infections,⁶⁹ was susceptible to all ApoB encrypted peptides (Figures 1B and 5B) and was thus utilized in our infection model. Upon induction of a skin infection in mice, a single dose of either (ri)-r(P)ApoB_S^{Pro} (at 20 or 200 μmol L⁻¹) or each of the three natural ApoB-derived encrypted peptides (at 200 μmol L⁻¹) was administered. Treatment with r(P)ApoB_L^{Pro}, r(P)ApoB_L^{Ala}, and r(P)ApoB_S^{Pro} (all at 200 μmol L⁻¹) significantly reduced *P. aeruginosa* colony-forming unit (CFU) counts by ~3 to 4 orders of magnitude after 4 days of treatment. We homogenized the tissue and quantified the bacterial load through CFU count assays as this quantitative method accurately reflects the number of the bacteria present in a given infected area.⁷⁰ Similar results were obtained with our control peptide CATH-2. Importantly, treatment with (ri)-r(P)ApoB_S^{Pro} at a significantly lower dose (20 μmol L⁻¹) reduced bacterial loads by ~3 orders of magnitude, and treatment with a higher peptide concentration (200 μmol L⁻¹) completely sterilized the infection at 4 days post-treatment (Figure 6B). Peptide (ri)-r(P)ApoB_S^{Pro} exerted its anti-infective activity in a dose-dependent manner (Figure 6D). At 4 days post-treatment, the retro-inverso peptide reduced bacterial counts by 3 orders of magnitude at 20 and 50 μmol L⁻¹ (Figure 6D) and completely eradicated *P. aeruginosa* infections at concentrations higher than 100 μmol L⁻¹ (Figure 6D). No significant weight changes or any obvious inflammation events were detected during the treatment period, thus confirming the lack of toxicity of these peptides in our murine model (Figures 6C and S14). Altogether, our data demonstrate the promising anti-infective activity of (ri)-r(P)ApoB_S^{Pro} in a preclinical mouse model.

CONCLUSION

Antibiotic resistance is predicted to become the leading cause of death in our society reaffirming the need to discover antimicrobials derived from previously underexplored sources. Here, we characterize and demonstrate the anti-infective properties of three peptides encoded within human apolipoprotein B. In addition to their direct antimicrobial effects, the peptides potentiated the activity of conventional antibiotics against bacteria, thus revealing a potential role for these agents as adjuvants in classical antibiotic therapy. Importantly, contrary to existing antibiotics, the encrypted peptides did not readily select for bacterial resistance in our laboratory evolution assays. These molecules also displayed significant antibiofilm activity against a range of bacterial strains, including those particularly dangerous and classified as the ESKAPE pathogens. The peptides reduced biofilm biovolume, altered biofilm architecture, and induced cell death. Human ApoB-derived encrypted peptides did not exert toxicity against normal human skin cells and did not induce adverse inflammatory responses in human monocytes. A more stable retro-inverso variant, composed entirely of D-amino acids, was engineered to ensure efficacy against infections in mice and overall translatability. This strategy helped to overcome issues around susceptibility to proteolysis, which have traditionally hindered development of peptide- and protein-based therapies,⁷¹ therefore making this molecule more suitable for future preclinical and clinical studies. Our findings link human plasma and innate immunity and identify human blood as a previously underexplored source of antibiotics.

METHODS

Materials. Unless specified otherwise, all reagents used in the present study were purchased from Sigma-Merck (Milan, Italy).

Bacterial Strains and Growth Conditions. All bacterial strains used in the analyses [i.e., *S. epidermidis* ATCC 35984, *S. aureus* ATCC 12600, *A. baumannii* ATCC 17878, *K. pneumoniae* ATCC 700603, *S. aureus* MRSA (WK7-2), *E. faecalis* ATCC 29212, and *P. aeruginosa* PAO1] were grown in the same media and experimental conditions as previously reported.^{6,7,72}

Peptides. Expression and isolation of recombinant peptides were carried out as previously described.²⁰ CATH-2 and (ri)-r(P)ApoB_S^{Pro} peptides were obtained from CPC Scientific Inc. (Sunnyvale, CA) and CASLO ApS (Kongens Lyngby, Denmark), respectively.

Antimicrobial Activity. The antimicrobial activity of ApoB-derived encrypted peptides was assessed against a panel of skin pathogens, such as *S. epidermidis* ATCC 35984, *S. aureus* ATCC 12600, *A. baumannii* ATCC 17878, *K. pneumoniae* ATCC 700603, *S. aureus* MRSA (WK7-2), *E. faecalis* ATCC 29212, and *P. aeruginosa* PAO1 by using the broth microdilution method.²¹ Bacteria were grown to midlogarithmic phase in MHB at 37 °C. Then, cells were diluted to 4 × 10⁶ CFU/mL in Difco 0.5× Nutrient Broth (Becton-Dickenson, Franklin Lakes, NJ) and mixed at a ratio of 1:1 v/v with 2-fold serial dilutions of peptides (0–40 μmol L⁻¹). Following incubation overnight, each sample was diluted, plated on TSA, and incubated at 37 °C for 24 h to count the number of colonies. All experiments were carried out in three independent replicates.

Antimicrobial Activity of Peptides upon Preincubation in 10% Serum. The antimicrobial activity of r(P)ApoB_S^{Pro} and (ri)-r(P)ApoB_S^{Pro} was evaluated against four bacterial strains upon preincubation in 10% FBS (fetal bovine serum, Microgem Lab, Cat. S1860, Italy). All the peptides were incubated for 1 or 16 h in serum at 37 °C (water bath) prior to MIC value determination by standard protocols.²¹ Experiments were carried out in triplicate for each peptide.

Stability Assay. The assay for resistance to enzymatic degradation was carried out according to the method described by Powell et al.⁷³ Briefly, peptides at 2 mg mL⁻¹ were exposed to a solution of 25% fetal bovine serum in water. Aliquots were collected after 0.5, 1, 2, and 4 h, and 10 μL of trifluoroacetic acid was added to them while the samples were on ice for 10 min. The enzymatic degradation of peptides was monitored by reverse-phase high-performance liquid chromatography coupled to mass spectrometry (RP-HPLC/ESI-MS). The area under the curve was used as a proxy for calculating the remaining peptide after exposure to enzymes from FBS. The percentage of peptide left was calculated by the following equation: [Peptide]_{remaining} = 100 × $\frac{AUC_t}{AUC_0}$, where AUC_t is the area under the curve of the peak related to the peptide after *t* h (*t* = 0.5, 1, 2, and 4 h) and AUC₀ is the area under the curve of the peak related to the peptide at the beginning of the experiment. Three independent experimental replicates were carried out, as previously described.⁷⁴

DiSC₃(5) Assay. Three independent cytoplasmic membrane depolarization assays were carried out on *S. epidermidis* ATCC 35984, *S. aureus* ATCC 12600, *A. baumannii* ATCC 17878 and *K. pneumoniae* ATCC 700603 using the 3,3'-dipropylthiadicarbocyanine iodide (diSC₃-5, TCI America), which is a membrane potential-sensitive dye.³⁴ Bacterial cells were grown to midlogarithmic phase and then washed and resuspended in 5 mmol L⁻¹ HEPES buffer (pH 7.2) containing 0.1 mol L⁻¹ KCl and 20 mmol L⁻¹ glucose at a density corresponding to an optical value at 600 nm of 0.06–0.03. The cell suspension was then incubated with 1 μmol L⁻¹ diSC₃(5) for 45 min to stabilize the fluorescence, and then the peptides were added to bacterial suspensions at concentrations corresponding to their MIC. Changes in fluorescence intensity were continuously recorded by using GloMax Discover System (Promega, Madison, WI), with excitation and emission wavelengths of 620 and 670 nm, respectively.

NPN Assay. The outer-membrane permeability 1-N-phenyl-naphthylamine (NPN) uptake assay was carried out using the Gram-negative pathogens *A. baumannii* ATCC 17878 and *K. pneumoniae* ATCC 700603. Bacterial cells were grown to midlogar-

ithmic phase and then washed and resuspended in 5 mmol L⁻¹ HEPES buffer (pH 7.2) at a density corresponding to an optical value at 600 nm of 0.4. Cell suspensions were incubated with each peptide at a concentration corresponding to its MIC value after which 4 μL of NPN solution (0.5 mmol L⁻¹; working concentration of 10 μmol L⁻¹ after dilutions) was added. Changes in fluorescence intensity were continuously recorded by using a GloMax Discover System (Promega, Madison, WI), with excitation and emission wavelengths of 350 and 420 nm, respectively. Membrane permeability assays were independently carried out three times.

Checkerboard Assay and Definition of Fractional Inhibitory Concentration (FIC) Index. Combinations of ApoB-derived encrypted peptides and antimicrobial agents were tested on *S. epidermidis* ATCC 35984, *S. aureus* ATCC 12600, *A. baumannii* ATCC 17878, and *K. pneumoniae* ATCC 700603 by the so-called “checkerboard” assay to determine the FIC indexes. To this purpose, 2-fold serial dilutions of each peptide were tested in combination with 2-fold serial dilutions of peptide, EDTA or antibiotics widely used in topical formulations (*i.e.*, vancomycin, erythromycin, colistin, polymyxin B, fusidic acid, clindamycin, gentamicin, and benzoyl peroxide). The FIC indexes of the two-drug combinations were calculated as follows: FIC_A + FIC_B, where FIC_A = $\frac{\text{MIC}_{\text{A-combination}}}{\text{MIC}_{\text{A-alone}}}$, and FIC_B = $\frac{\text{MIC}_{\text{B-combination}}}{\text{MIC}_{\text{B-alone}}}$. In the case of the three-drug combinations, we measured the effects of the third drug FIC_C = $\frac{\text{MIC}_{\text{C-combination}}}{\text{MIC}_{\text{C-alone}}}$ added to the previous two drugs combined (A + B). The FIC indexes of the three-drug interactions were calculated as follows: $\frac{(\text{FIC}_A + \text{FIC}_C) + (\text{FIC}_B + \text{FIC}_C)}{2}$. FIC indexes of ≤0.5 were classified as synergism, while FIC indexes between 0.5 and 1 or between 1 and 4 were associated with additive and indifferent effects, respectively.⁶

Scanning Electron Microscopy Analyses. To carry out SEM analyses, *K. pneumoniae* ATCC 700603 (2 × 10⁸ CFU/mL) was incubated with 0.58 μmol L⁻¹ r(P)ApoB_S^{Pro} in combination with 0.36 μmol mL⁻¹ colistin for 3 h at 37 °C. Following incubation, the samples were processed and characterized as previously reported.⁷⁵

Killing Kinetic Studies. To kinetically analyze the antibacterial effects of ApoB-derived encrypted peptides coadministered with conventional antibiotics (*e.g.*, colistin and polymyxin B), experiments were carried out using *K. pneumoniae* ATCC 700603 treated with a combination of both antimicrobials or with the single agents at concentrations corresponding to their MIC. Bacterial cells were diluted to 4 × 10⁶ CFU/mL in Difco 0.5× Nutrient Broth and mixed at a ratio of 1:1 v/v with the peptide, the antibiotic, or both. At defined time points, samples were serially diluted, and each dilution was plated on tryptic soy agar. Following an incubation of 20 h at 37 °C, colonies were counted.

Bacterial Resistance Development Assay. *S. epidermidis* ATCC 35984, *S. aureus* ATCC 12600, and *A. baumannii* ATCC 17878 bacterial strains were exposed to colistin, gentamicin, mupirocin, r(P)ApoB_L^{Pro}, r(P)ApoB_L^{Ala}, or r(P)ApoB_S^{Pro}. Once we detected the MIC values for each peptide or antibiotic against the bacterial strains tested, we transferred bacterial cells that survived exposure at a subinhibitory (MIC/2) concentration, and they were regrown and re-exposed to the respective peptide or antibiotic.²¹ The treatment was repeated for 30 days. Strains that developed resistance to antibiotics presented higher MICs at subsequent passages, and the cells from the last passage were isolated and stored for scanning electron microscopy analyses.

Antibiofilm Activity Assays. Antibiofilm activity assays were carried out on *S. epidermidis* ATCC 35984, *S. aureus* ATCC 12600, *A. baumannii* ATCC 17878, and *K. pneumoniae* ATCC 700603. Bacteria were grown overnight at 37 °C and then diluted to 4 × 10⁸ CFU/mL in 0.5× MHB medium. Incubations with increasing concentrations of each peptide (0–40 μmol L⁻¹) were carried out, as previously described^{6,76} for either 4 or 24 h to test peptide effects on cell attachment or on biofilm formation, respectively. Instead, to evaluate the effect of peptides on preformed biofilm, a bacterial biofilm was formed for 24 h at 37 °C and subsequently treated with the peptides.

Crystal violet assays and confocal laser scanning microscopy analyses in static conditions were carried out according to the method described by Gaglione *et al.*^{6,77}

Eukaryotic Cell Culture and Cytotoxicity Assays. Immortalized human keratinocytes (HaCaT), human epidermoid carcinoma cells (A431), and human dermal fibroblasts (HDF) were cultured in high-glucose Dulbecco's modified Eagle's medium (DMEM) supplemented with 10% fetal bovine serum (FBS), 1% antibiotics (Pen/strep), and 1% L-glutamine. THP-1 cells obtained from ATCC (American Type Culture Collection: TIB-202) were cultured in suspension in RPMI containing Glutamax supplemented with 10% (v/v) FBS. All cell lines were grown at 37 °C in a humidified atmosphere containing 5% CO₂. Cells were seeded on 96-well plates at a density of 3 × 10³ cells/well at 24 h prior to treatment, then incubated in the presence of increasing peptide concentrations (0–200 μmol L⁻¹) for 24, 48, and 72 h. Following treatment with peptides, MTT assays were carried out as previously described.^{6,77,78} Briefly, cell culture supernatants were replaced with 0.5 mg/mL MTT reagent dissolved in DMEM medium without red phenol (100 μL/well). After 4 h of incubation at 37 °C, the resulting insoluble formazan salts were solubilized in 0.04 M HCl in anhydrous isopropanol and quantified using an automatic plate reader spectrophotometer (Synergy H4 Hybrid Microplate Reader, BioTek Instruments, Inc., Winooski, VT) by measuring the absorbance at 570 nm. Cell viability was expressed as means of the percentage values compared to control untreated cells. Lactate dehydrogenase (LDH) secretion in culture medium was measured by using Lactate Dehydrogenase Activity Assay Kit (TOX7; Sigma) according to the manufacturer's instructions. At the end of cell treatment, aliquots of supernatants were collected and added to a reaction mix containing Lactate Assay Buffer, Lactate Enzyme Mix, and Lactate Substrate Mix. Absorbance at 490 nm was determined for each sample using an automatic plate reader spectrophotometer. The positive control was obtained by treating cells with lysis buffer provided by the manufacturer.

Gene Expression Studies. Human dermal fibroblasts were seeded into 24-well plates at a density of 1.5 × 10⁴ cells/well. After 24 h, the culture medium was replaced with fresh DMEM (negative control), *S. aureus* or *A. baumannii* culture at multiplicity of infection (MOI) of 0.01, and LPS from *E. coli* O55:B5 or LTA from *S. aureus* (S6411–57–5; Sigma) at 1 μg mL⁻¹, and the samples were treated with each ApoB-derived encrypted peptide (5, 10, or 20 μmol L⁻¹) or with CATH-2 (2.5 or 5 μmol L⁻¹). Total RNA was extracted by using Trizol (Ambion, Carlsbad, CA) reagent according to the manufacturer's instructions. The iScript cDNA synthesis kit (Bio-Rad, Veenendaal, The Netherlands) was used to reverse-transcribe all RNA samples. Quantitative real-time PCR (qRT-PCR) was then carried out to evaluate mRNA expression by using manufacturer's protocol (iQ SYBR Green Supermix - Bio-Rad). Reactions were carried out by using the following primer sequences: IL-8, 5'-CTGGCCGTGGCTCTCTTG-3' (sense) and 5'-CCTTGG-CAAAACTGCACCTT-3' (antisense); IL-6, 5'-TGCAA-TAACACCCCTGACC-3' (sense) and 5'-TGCGCAGAATGAGATGAGTTG-3' (antisense); and β-actin, 5'-ATGTGGATCAGCAAG-CAGGAGTA-3' (sense) and 5'-GCATTTCGGTGGACGAT-3' (antisense). The β-actin mRNA was used as an internal control to normalize the expression of the target genes.

Enzyme-Linked Immunosorbent Assay (ELISA). To evaluate possible pro-inflammatory effects exerted by ApoB-derived encrypted peptides, THP-1 cells, upon treatment with 100 μmol L⁻¹ phorbol 12-myristate 13-acetate (PMA) for 3 days, were plated into 96-well plates at a density of 3 × 10³ cells/well in 100 μL of medium. Following incubation with peptides, cytokines levels within the medium were quantified by using human immunoassay kits (DuoSet ELISA kits, R&D Systems, Minneapolis, MN) according to the manufacturer's instructions. An ELISA reader set to 450 nm with a wavelength correction set to 540 nm was used to measure the optical density of each sample.

Histone Deacetylase Enzyme (HDAC) Assay. Human keratinocytes were treated with 20 μmol L⁻¹ each ApoB-derived

peptide or with 50 nmol L⁻¹ Tricostatin A for 30 min. The effects on HDAC activity were then evaluated by using HDAC-Glo I/II Assays and Screening System (Promega) according to the manufacturer's instructions.

Scarification Skin Infection Mouse Model. The anti-infective properties of ApoB-derived encrypted peptides (at working concentrations of 20, 50, 100, 150, or 200 μmol L⁻¹) were assessed in a skin murine model infected with the *P. aeruginosa* strain PAO1 as previously described by Pane et al.^{4,7,9,10} Two independent experiments were carried out with 4 mice per group. Statistical significance was assessed using a one-way ANOVA.

ASSOCIATED CONTENT

Supporting Information

The Supporting Information is available free of charge at <https://pubs.acs.org/doi/10.1021/acsnano.1c04496>.

Antimicrobial activity of ApoB encrypted peptides and antibiotics, antimicrobial effects of peptides combined each other or with traditional antimicrobials, SEM images of the most promising combinatory therapy, exact MIC values for ApoB encrypted peptides and conventional antimicrobial agents, Gram-negative bacteria outer-membrane permeabilization assay results, resistance development studies using *S. aureus* ATCC 12600, antimicrobial effects of ApoB-derived encrypted peptides in 2- and 3-way combinations, determination of the minimal biofilm inhibitory concentration of the ApoB-derived peptides by crystal violet assays, anti-biofilm properties of encrypted peptides against *A. baumannii* strain under static conditions, biocompatibility analyses of ApoB-derived encrypted peptides at 25, 50, 100, and 200 μmol L⁻¹, analyses of anti-inflammatory effects in Gram-negative and LPS-mediated inflammation, immunomodulatory effects on THP-1 cells induced by ApoB encrypted peptides, antimicrobial activity of (ri)-r(P)ApoB_S^{Pro}, exact MIC values of the synthetic peptide, biocompatibility analyses of (ri)-r(P)ApoB_S^{Pro} at 25, 50, 100, and 200 μmol L⁻¹, and mouse body weight changes throughout the duration of the experiment (PDF)

AUTHOR INFORMATION

Corresponding Authors

Cesar de la Fuente-Nunez – Machine Biology Group, Departments of Psychiatry and Microbiology, Institute for Biomedical Informatics, Institute for Translational Medicine and Therapeutics, Perelman School of Medicine and Departments of Bioengineering and Chemical and Biomolecular Engineering, School of Engineering and Applied Science, University of Pennsylvania, Philadelphia, Pennsylvania 19104, United States; Penn Institute for Computational Science, University of Pennsylvania, Philadelphia, Pennsylvania 19104, United States; orcid.org/0000-0002-2005-5629; Email: cfuente@upenn.edu

Angela Arciello – Department of Chemical Sciences, University of Naples Federico II, Naples I-80126, Italy; Istituto Nazionale di Biostrutture e Biosistemi (INBB), Rome 00136, Italy; orcid.org/0000-0001-8269-6459; Email: anarciel@unina.it

Authors

Angela Cesaro – Department of Chemical Sciences, University of Naples Federico II, Naples I-80126, Italy; Department of

Biomolecular Health Sciences, Division of Infectious Diseases and Immunology, Section Molecular Host Defence, Faculty of Veterinary Medicine, Utrecht University, Utrecht 3584 CL, The Netherlands; Machine Biology Group, Departments of Psychiatry and Microbiology, Institute for Biomedical Informatics, Institute for Translational Medicine and Therapeutics, Perelman School of Medicine and Departments of Bioengineering and Chemical and Biomolecular Engineering, School of Engineering and Applied Science, University of Pennsylvania, Philadelphia, Pennsylvania 19104, United States; Penn Institute for Computational Science, University of Pennsylvania, Philadelphia, Pennsylvania 19104, United States; orcid.org/0000-0003-0435-5346

Marcelo D. T. Torres – Machine Biology Group, Departments of Psychiatry and Microbiology, Institute for Biomedical Informatics, Institute for Translational Medicine and Therapeutics, Perelman School of Medicine and Departments of Bioengineering and Chemical and Biomolecular Engineering, School of Engineering and Applied Science, University of Pennsylvania, Philadelphia, Pennsylvania 19104, United States; Penn Institute for Computational Science, University of Pennsylvania, Philadelphia, Pennsylvania 19104, United States; orcid.org/0000-0002-6165-9138

Rosa Gaglione – Department of Chemical Sciences, University of Naples Federico II, Naples I-80126, Italy; Istituto Nazionale di Biostrutture e Biosistemi (INBB), Rome 00136, Italy; orcid.org/0000-0003-2391-0237

Eliana Dell'Olmo – Department of Chemical Sciences, University of Naples Federico II, Naples I-80126, Italy; orcid.org/0000-0002-4298-5683

Rocco Di Girolamo – Department of Chemical Sciences, University of Naples Federico II, Naples I-80126, Italy; orcid.org/0000-0001-8815-2997

Andrea Bosso – Department of Biology, University of Naples Federico II, Naples I-80126, Italy; orcid.org/0000-0003-2360-300X

Elio Pizzo – Department of Biology, University of Naples Federico II, Naples I-80126, Italy; orcid.org/0000-0002-3652-8865

Henk P. Haagsman – Department of Biomolecular Health Sciences, Division of Infectious Diseases and Immunology, Section Molecular Host Defence, Faculty of Veterinary Medicine, Utrecht University, Utrecht 3584 CL, The Netherlands; orcid.org/0000-0002-4931-5201

Edwin J. A. Veldhuizen – Department of Biomolecular Health Sciences, Division of Infectious Diseases and Immunology, Section Immunology, Faculty of Veterinary Medicine, Utrecht University, Utrecht 3584 CL, The Netherlands; orcid.org/0000-0002-9133-7965

Complete contact information is available at: <https://pubs.acs.org/doi/10.1021/acsnano.1c04496>

Author Contributions

A.C., C.F.-N., and A.A. conceived the idea and designed the project. C.F.-N. and A.A. supervised, administered, and managed the project. A.C. designed and conducted most of the experiments. R.G., E.D.O., R.D.G., A.B., and E.P. conducted specific experiments. H.P.H. and E.J.A.V. provided expertise for the analysis of peptides' biocompatibility and anti-inflammatory effects. A.C. and M.D.T.T. designed the

synthetic version of the peptide and carried out the animal model experiments. A.C., M.D.T.T., C.F.-N., and A.A. wrote the paper. All the authors revised the manuscript.

Notes

The authors declare no competing financial interest.

ACKNOWLEDGMENTS

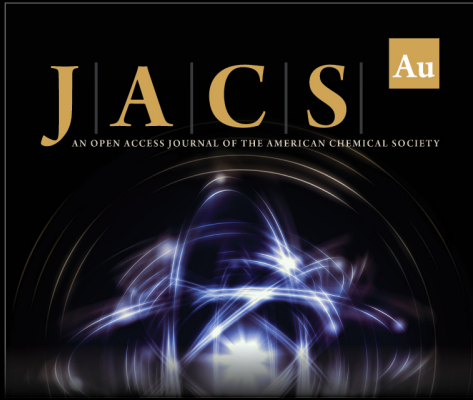
C.F.-N. holds a Presidential Professorship at the University of Pennsylvania, is a recipient of the Langer Prize by the AICHE Foundation, and acknowledges funding from the Institute for Diabetes, Obesity, and Metabolism, the Penn Mental Health AIDS Research Center of the University of Pennsylvania, the Nemirovsky Prize, and the Dean's Innovation Fund from the Perelman School of Medicine at the University of Pennsylvania. Research reported in this publication was supported by the National Institute of General Medical Sciences of the National Institutes of Health under award number R35GM138201, the Defense Threat Reduction Agency (DTRA; HDTRA11810041 and HDTRA1-21-1-0014), and by Programma Operativo Nazionale (PON) Ricerca e Innovazione 2014-2020 "Dottorati innovativi con caratterizzazione industriale".

REFERENCES

- (1) Santajit, S.; Indrawattana, N. Mechanisms of Antimicrobial Resistance in ESKAPE Pathogens. *BioMed. Research International* **2016**, *2016*, 1–8.
- (2) CDC. *Antibiotic/Antimicrobial Resistance (AR/AMR) Threats Report*. <https://www.cdc.gov/drugresistance/biggest-threats.html> (accessed 2021-12-27).
- (3) Mulani, M. S.; Kamble, E. E.; Kumkar, S. N.; Tawre, M. S.; Pardesi, K. R. Emerging Strategies to Combat ESKAPE Pathogens in the Era of Antimicrobial Resistance: A Review. *Frontiers in Microbiology* **2019**, *10*, 539.
- (4) Pfalzgraff, A.; Brandenburg, K.; Weindl, G. Antimicrobial Peptides and Their Therapeutic Potential for Bacterial Skin Infections and Wounds. *Front. Pharmacol.* **2018**, *9*, 00281.
- (5) Pane, K.; Sgambati, V.; Zanfardino, A.; Smaldone, G.; Cafaro, V.; Angrisano, T.; Pedone, E.; Di Gaetano, S.; Capasso, D.; Haney, E. F.; Izzo, V.; Varcamonti, M.; Notomista, E.; Hancock, R. E. W.; Di Donato, A.; Pizzo, E. A New Cryptic Cationic Antimicrobial Peptide from Human Apolipoprotein E with Antibacterial Activity and Immunomodulatory Effects on Human Cells. *FEBS Journal* **2016**, *283* (11), 2115–2131.
- (6) Gaglione, R.; Dell'Olmo, E.; Bosso, A.; Chino, M.; Pane, K.; Ascione, F.; Itri, F.; Caserta, S.; Amoresano, A.; Lombardi, A.; Haagsman, H. P.; Piccoli, R.; Pizzo, E.; Veldhuizen, E. J. A.; Notomista, E.; Arciello, A. Novel Human Bioactive Peptides Identified in Apolipoprotein B: Evaluation of Their Therapeutic Potential. *Biochem. Pharmacol.* **2017**, *130*, 34–50.
- (7) Torres, M. D. T.; Melo, M. C. R.; Crescenzi, O.; Notomista, E.; de la Fuente-Nunez, C. Mining for Encrypted Peptide Antibiotics in the Human Proteome. *Nat. Biomed. Eng.* **2021**. DOI: 10.1038/s41551-021-00801-1.
- (8) Gaglione, R.; Pizzo, E.; Notomista, E.; de la Fuente-Nunez, C.; Arciello, A. Host Defence Cryptides from Human Apolipoproteins: Applications in Medicinal Chemistry. *Current Topics in Medicinal Chemistry* **2020**, *20* (14), 1324–1337.
- (9) Pane, K.; Cafaro, V.; Avitabile, A.; Torres, M. D. T.; Vollaro, A.; De Gregorio, E.; Catania, M. R.; Di Maro, A.; Bosso, A.; Gallo, G.; Zanfardino, A.; Varcamonti, M.; Pizzo, E.; Di Donato, A.; Lu, T. K.; de la Fuente-Nunez, C.; Notomista, E. Identification of Novel Cryptic Multifunctional Antimicrobial Peptides from the Human Stomach Enabled by a Computational–Experimental Platform. *ACS Synth. Biol.* **2018**, *7* (9), 2105–2115.
- (10) Autelitano, D. J.; Rajic, A.; Smith, A. I.; Berndt, M. C.; Ilag, L. L.; Vadas, M. The Cryptome: A Subset of the Proteome, Comprising Cryptic Peptides with Distinct Bioactivities. *Drug Discovery Today* **2006**, *11*, 306.
- (11) Ueki, N.; Someya, K.; Matsuo, Y.; Wakamatsu, K.; Mukai, H. Cryptides: Functional Cryptic Peptides Hidden in Protein Structures. *Biopolymers* **2007**, *88* (2), 190–198.
- (12) Gaglione, R.; Dell'Olmo, E.; Bosso, A.; Chino, M.; Pane, K.; Ascione, F.; Itri, F.; Caserta, S.; Amoresano, A.; Lombardi, A.; Haagsman, H. P.; Piccoli, R.; Pizzo, E.; Veldhuizen, E. J. A.; Notomista, E.; Arciello, A. Novel Human Bioactive Peptides Identified in Apolipoprotein B: Evaluation of Their Therapeutic Potential. *Biochemical pharmacology* **2017**, *130*, 34–50.
- (13) Pane, K.; Sgambati, V.; Zanfardino, A.; Smaldone, G.; Cafaro, V.; Angrisano, T.; Pedone, E.; Di Gaetano, S.; Capasso, D.; Haney, E. F.; Izzo, V.; Varcamonti, M.; Notomista, E.; Hancock, R. E. W.; Di Donato, A.; Pizzo, E. A New Cryptic Cationic Antimicrobial Peptide from Human Apolipoprotein E with Antibacterial Activity and Immunomodulatory Effects on Human Cells. *FEBS Journal* **2016**, *283* (11), 2115–2131.
- (14) Gaglione, R.; Cesaro, A.; Dell'Olmo, E.; Della Ventura, B.; Casillo, A.; Di Girolamo, R.; Velotta, R.; Notomista, E.; Veldhuizen, E. J. A.; Corsaro, M. M.; De Rosa, C.; Arciello, A. Effects of Human Antimicrobial Cryptides Identified in Apolipoprotein B Depend on Specific Features of Bacterial Strains. *Sci. Rep.* **2019**, *9* (1), 6728.
- (15) Shapiro, M. D.; Fazio, S. Apolipoprotein B-Containing Lipoproteins and Atherosclerotic Cardiovascular Disease. *F1000Research* **2017**, *6*, 134.
- (16) Lister, P. D.; Wolter, D. J.; Hanson, N. D. Antibacterial-Resistant *Pseudomonas Aeruginosa*: Clinical Impact and Complex Regulation of Chromosomally Encoded Resistance Mechanisms. *Clin. Microbiol. Rev.* **2009**, *22* (4), 582–610.
- (17) Welty, F. K.; Lichtenstein, A. H.; Barrett, P. H. R.; Dolnikowski, G. G.; Schaefer, E. J. Human Apolipoprotein (Apo) B-48 and ApoB-100 Kinetics with Stable Isotopes. *Arterioscler., Thromb., Vasc. Biol.* **1999**, *19* (12), 2966–2974.
- (18) Han, R. Plasma Lipoproteins Are Important Components of the Immune System. *Microbiol. Immunol.* **2010**, *54* (4), 246–253.
- (19) Pane, K.; Durante, L.; Crescenzi, O.; Cafaro, V.; Pizzo, E.; Varcamonti, M.; Zanfardino, A.; Izzo, V.; Di Donato, A.; Notomista, E. Antimicrobial Potency of Cationic Antimicrobial Peptides Can Be Predicted from Their Amino Acid Composition: Application to the Detection of "Cryptic" Antimicrobial Peptides. *J. Theor. Biol.* **2017**, *419*, 254–265.
- (20) Gaglione, R.; Pane, K.; Dell'Olmo, E.; Cafaro, V.; Pizzo, E.; Olivieri, G.; Notomista, E.; Arciello, A. Cost-Effective Production of Recombinant Peptides in *Escherichia Coli*. *New Biotechnology* **2019**, *51*, 39–48.
- (21) Wiegand, I.; Hilpert, K.; Hancock, R. E. W. Agar and Broth Dilution Methods to Determine the Minimal Inhibitory Concentration (MIC) of Antimicrobial Substances. *Nature protocols* **2008**, *3* (2), 163–175.
- (22) Rahnamaian, M.; Vilcinskas, A. Short Antimicrobial Peptides as Cosmetic Ingredients to Deter Dermatological Pathogens. *Appl. Microbiol. Biotechnol.* **2015**, *99* (21), 8847–8855.
- (23) Wu, X.; Hurdle, J. G. Screening for a Diamond in the Rough. *Chemistry & Biology* **2013**, *20* (9), 1091–1092.
- (24) te Winkel, J. D.; Gray, D. A.; Seistrup, K. H.; Hamoen, L. W.; Strahl, H. Analysis of Antimicrobial-Tripped Membrane Depolarization Using Voltage Sensitive Dyes. *Front. Cell Dev. Biol.* **2016**, *4*, 00029 DOI: 10.3389/fcell.2016.00029.
- (25) van Dijk, A.; van Eldik, M.; Veldhuizen, E. J. A.; Tjeerdsma-van Bokhoven, H. L. M.; de Zoete, M. R.; Bikker, F. J.; Haagsman, H. P. Immunomodulatory and Anti-Inflammatory Activities of Chicken Cathelicidin-2 Derived Peptides. *PLoS One* **2016**, *11* (2), No. e0147919.
- (26) van Dijk, A.; Molhoek, E. M.; Veldhuizen, E. J. A.; Bokhoven, J. L. M. T. T.; Wagendorp, E.; Bikker, F.; Haagsman, H. P. Identification of Chicken Cathelicidin-2 Core Elements Involved in Antibacterial and Immunomodulatory Activities. *Molecular Immunology* **2009**, *46* (13), 2465–2473.


- (27) Boix-Lemonche, G.; Lekka, M.; Skerlavaj, B. A Rapid Fluorescence-Based Microplate Assay to Investigate the Interaction of Membrane Active Antimicrobial Peptides with Whole Gram-Positive Bacteria. *Antibiotics* **2020**, *9* (2), 92.
- (28) Murugan, R. N.; Jacob, B.; Ahn, M.; Hwang, E.; Sohn, H.; Park, H.-N.; Lee, E.; Seo, J.-H.; Cheong, C.; Nam, K.-Y.; Hyun, J.-K.; Jeong, K.-W.; Kim, Y.; Shin, S. Y.; Bang, J. K. De Novo Design and Synthesis of Ultra-Short Peptidomimetic Antibiotics Having Dual Antimicrobial and Anti-Inflammatory Activities. *PLoS One* **2013**, *8* (11), No. e80025.
- (29) Gao, W.; Xing, L.; Qu, P.; Tan, T.; Yang, N.; Li, D.; Chen, H.; Feng, X. Identification of a Novel Cathelicidin Antimicrobial Peptide from Ducks and Determination of Its Functional Activity and Antibacterial Mechanism. *Sci. Rep.* **2015**, *5*, 17260.
- (30) Zhang, L.; Dhillon, P.; Yan, H.; Farmer, S.; Hancock, R. E. W. Interactions of Bacterial Cationic Peptide Antibiotics with Outer and Cytoplasmic Membranes of *Pseudomonas Aeruginosa*. *Antimicrob. Agents Chemother.* **2000**, *44* (12), 3317.
- (31) Hou, J.; Liu, Z.; Cao, S.; Wang, H.; Jiang, C.; Hussain, M. A.; Pang, S. Broad-Spectrum Antimicrobial Activity and Low Cytotoxicity against Human Cells of a Peptide Derived from Bovine ASI-Casein. *Molecules* **2018**, *23* (5), 1220.
- (32) Berditsch, M.; Jäger, T.; Stempel, N.; Schwartz, T.; Overhage, J.; Ulrich, A. S. Synergistic Effect of Membrane-Active Peptides Polymyxin B and Gramicidin S on Multidrug-Resistant Strains and Biofilms of *Pseudomonas Aeruginosa*. *Antimicrob. Agents Chemother.* **2015**, *59* (9), 5288–5296.
- (33) Reffuveille, F.; de la Fuente-Núñez, C.; Mansour, S.; Hancock, R. E. W. A Broad-Spectrum Antibiofilm Peptide Enhances Antibiotic Action against Bacterial Biofilms. *Antimicrob. Agents Chemother.* **2014**, *58* (9), 5363–5371.
- (34) Thappeta, K. R. v.; Vikhe, Y. S.; Yong, A. M. H.; Chan-Park, M. B.; Kline, K. A. Combined Efficacy of an Antimicrobial Cationic Peptide Polymer with Conventional Antibiotics to Combat Multi-drug-Resistant Pathogens. *ACS Infectious Diseases* **2020**, *6* (5), 1228–1237.
- (35) de la Fuente-Núñez, C.; Reffuveille, F.; Mansour, S. C.; Reckseidler-Zenteno, S. L.; Hernández, D.; Brackman, G.; Coenye, T.; Hancock, R. E. W. D-Enantiomeric Peptides That Eradicate Wild-Type and Multidrug-Resistant Biofilms and Protect against Lethal *Pseudomonas Aeruginosa* Infections. *Chemistry & Biology* **2015**, *22* (2), 196–205.
- (36) Silva, O. N.; Torres, M. D. T.; Cao, J.; Alves, E. S. F.; Rodrigues, L. v.; Resende, J. M.; Lião, L. M.; Porto, W. F.; Fensterseifer, I. C. M.; Lu, T. K.; Franco, O. L.; de la Fuente-Núñez, C. Repurposing a Peptide Toxin from Wasp Venom into Anti-infectives with Dual Antimicrobial and Immunomodulatory Properties. *Proc. Natl. Acad. Sci. U.S.A.* **2020**, *117* (43), 26936.
- (37) Wilson, H. L.; Daveson, K.; del Mar, C. B. Optimal Antimicrobial Duration for Common Bacterial Infections. *Australian Prescriber* **2019**, *42* (1), 5.
- (38) Torres, M. D. T.; Cao, J.; Franco, O. L.; Lu, T. K.; de la Fuente-Núñez, C. Synthetic Biology and Computer-Based Frameworks for Antimicrobial Peptide Discovery. *ACS Nano* **2021**, *15* (2), 2143–2164.
- (39) Torres, M. D. T.; Sothiselvam, S.; Lu, T. K.; de la Fuente-Núñez, C. Peptide Design Principles for Antimicrobial Applications. *J. Mol. Biol.* **2019**, *431*, 3547.
- (40) Prada-Prada, S.; Flórez-Castillo, J.; Farfán-García, A.; Guzmán, F.; Hernández-Peñaranda, I. Antimicrobial Activity of Ib-M Peptides against *Escherichia Coli* O157: H7. *PLoS One* **2020**, *15* (2), No. e0229019.
- (41) Brudzynski, K.; Sjaarda, C. Honey Glycoproteins Containing Antimicrobial Peptides, Jelleins of the Major Royal Jelly Protein 1, Are Responsible for the Cell Wall Lytic and Bactericidal Activities of Honey. *PLoS One* **2015**, *10* (4), No. e0120238.
- (42) el Shazely, B.; Yu, G.; Johnston, P. R.; Rolff, J. Resistance Evolution against Antimicrobial Peptides in *Staphylococcus Aureus* Alters Pharmacodynamics Beyond the MIC. *Front. Microbiol.* **2020**, *11*, 00103 DOI: 10.3389/fmicb.2020.00103.
- (43) Crouzet, M.; le Senechal, C.; Brözel, V. S.; Costaglioli, P.; Barthe, C.; Bonneau, M.; Garbay, B.; Vilain, S. Exploring Early Steps in Biofilm Formation: Set-Up of an Experimental System for Molecular Studies. *BMC Microbiology* **2014**, *14* (1), 253.
- (44) de la Fuente-Núñez, C.; Korolik, V.; Bains, M.; Nguyen, U.; Breidenstein, E. B. M.; Horsman, S.; Lewenza, S.; Burrows, L.; Hancock, R. E. W. Inhibition of Bacterial Biofilm Formation and Swarming Motility by a Small Synthetic Cationic Peptide. *Antimicrob. Agents Chemother.* **2012**, *56* (5), 2696.
- (45) Perry, J. A.; Wright, G. D. Forces Shaping the Antibiotic Resistome. *BioEssays* **2014**, *36* (12), 1179–1184.
- (46) Fujita, Y.; Taguchi, H. Current Status of Multiple Antigen-Presenting Peptide Vaccine Systems: Application of Organic and Inorganic Nanoparticles. *Chemistry Central Journal* **2011**, *5* (1), 48.
- (47) Veas, F.; Dubois, G. IL-22 Induces an Acute-Phase Response Associated to a Cohort of Acute Phase Proteins and Antimicrobial Peptides as Players of Homeostasis. In *Acute Phase Proteins - Regulation and Functions of Acute Phase Proteins*; InTech, 2011. DOI: 10.5772/20386.
- (48) Wang, C.; Tian, L.-L.; Li, S.; Li, H.-B.; Zhou, Y.; Wang, H.; Yang, Q.-Z.; Ma, L.-J.; Shang, D.-J. Rapid Cytotoxicity of Antimicrobial Peptide Tempoprin-ICEa in Breast Cancer Cells through Membrane Destruction and Intracellular Calcium Mechanism. *PLoS One* **2013**, *8* (4), No. e60462.
- (49) Tornesello, A. L.; Borrelli, A.; Buonaguro, L.; Buonaguro, F. M.; Tornesello, M. L. Antimicrobial Peptides as Anticancer Agents: Functional Properties and Biological Activities. *Molecules*. **2020**, *25*, 2850.
- (50) Pedron, C. N.; de Oliveira, C. S.; da Silva, A. F.; Andrade, G. P.; da Silva Pinhal, M. A.; Cerchiaro, G.; da Silva Junior, P. I.; da Silva, F. D.; Torres, M. D. T.; Oliveira, V. X. The Effect of Lysine Substitutions in the Biological Activities of the Scorpion Venom Peptide VmCT1. *Eur. J. Pharm. Sci.* **2019**, *136*, 104952.
- (51) Lu, Y.; Zhang, T.-F.; Shi, Y.; Zhou, H.-W.; Chen, Q.; Wei, B.-Y.; Wang, X.; Yang, T.-X.; Chinn, Y. E.; Kang, J.; Fu, C.-Y. PFR Peptide, One of the Antimicrobial Peptides Identified from the Derivatives of Lactoferrin, Induces Necrosis in Leukemia Cells. *Sci. Rep.* **2016**, *6* (1), 20823.
- (52) Méndez-Samperio, P. Recent Advances in the Field of Antimicrobial Peptides in Inflammatory Diseases. *Advanced Biomedical Research* **2013**, *2* (1), 50.
- (53) Haisma, E. M.; Rietveld, M. H.; de Breij, A.; van Dissel, J. T.; el Ghalbzouri, A.; Nibbering, P. H. Inflammatory and Antimicrobial Responses to Methicillin-Resistant *Staphylococcus Aureus* in an *In Vitro* Wound Infection Model. *PLoS One* **2013**, *8* (12), No. e82800.
- (54) Totté, J. E. E.; van der Feltz, W. T.; Bode, L. G. M.; van Belkum, A.; van Zuuren, E. J.; Pasmans, S. G. M. A. A Systematic Review and Meta-Analysis on *Staphylococcus Aureus* Carriage in Psoriasis, Acne and Rosacea. *European Journal of Clinical Microbiology & Infectious Diseases* **2016**, *35* (7), 1069–1077.
- (55) Hoffmann, J. P.; Friedman, J. K.; Wang, Y.; McLachlan, J. B.; Sammarco, M. C.; Morici, L. A.; Roy, C. J. *In Situ* Treatment with Novel Microbicide Inhibits Methicillin Resistant *Staphylococcus Aureus* in a Murine Wound Infection Model. *Front. Microbiol.* **2020**, *10*, 03106 DOI: 10.3389/fmicb.2019.03106.
- (56) Pietrzak, A.; Chabros, P.; Grywalska, E.; Kicinski, P.; Franciszkiewicz-Pietrzak, K.; Krasowska, D.; Kandzierski, G. Serum Lipid Metabolism in Psoriasis and Psoriatic Arthritis - An Update. *Archives of medical science: AMS* **2019**, *15* (2), 369–375.
- (57) Hall, P. R.; Elmore, B. O.; Spang, C. H.; Alexander, S. M.; Manifold-Wheeler, B. C.; Castleman, M. J.; Daly, S. M.; Peterson, M. M.; Sully, E. K.; Femling, J. K.; Otto, M.; Horswill, A. R.; Timmins, G. S.; Gresham, H. D. Nox2 Modification of LDL Is Essential for Optimal Apolipoprotein B-Mediated Control of Agr Type III *Staphylococcus Aureus* Quorum-Sensing. *PLoS Pathogens* **2013**, *9* (2), No. e1003166.


- (58) Pernot, M.; Vanderesse, R.; Frochot, C.; Guillemin, F.; Barberi-Heyob, M. Stability of Peptides and Therapeutic Success in Cancer. *Expert Opinion on Drug Metabolism & Toxicology* **2011**, *7* (7), 793–802.
- (59) Starr, C. G.; Wimley, W. C. Antimicrobial Peptides Are Degraded by the Cytosolic Proteases of Human Erythrocytes. *Biochimica et Biophysica Acta (BBA) - Biomembranes* **2017**, *1859* (12), 2319–2326.
- (60) Böttger, R.; Hoffmann, R.; Knappe, D. Differential Stability of Therapeutic Peptides with Different Proteolytic Cleavage Sites in Blood. *Plasma and Serum. PLOS ONE* **2017**, *12* (6), No. e0178943.
- (61) Garton, M.; Nim, S.; Stone, T. A.; Wang, K. E.; Deber, C. M.; Kim, P. M. Method to Generate Highly Stable D-Amino Acid Analogs of Bioactive Helical Peptides Using a Mirror Image of the Entire PDB. *Proc. Natl. Acad. Sci. U. S. A.* **2018**, *115* (7), 1505–1510.
- (62) Cardoso, M. H.; Cândido, E. S.; Oshiro, K. G. N.; Rezende, S. B.; Franco, O. L. Peptides Containing D-Amino Acids and Retro-Inverso Peptides. In *Peptide Applications in Biomedicine, Biotechnology and Bioengineering*; Elsevier, 2018; pp 131–155.
- (63) Oliva, R.; Chino, M.; Pane, K.; Pistorio, V.; De Santis, A.; Pizzo, E.; D'Errico, G.; Pavone, V.; Lombardi, A.; Del Vecchio, P.; Notomista, E.; Natri, F.; Petraccone, L. Exploring the Role of Unnatural Amino Acids in Antimicrobial Peptides. *Sci. Rep.* **2018**, *8* (1), 8888.
- (64) Torres, M. D. T.; Pedron, C. N.; Higashikuni, Y.; Kramer, R. M.; Cardoso, M. H.; Oshiro, K. G. N.; Franco, O. L.; Silva Junior, P. I.; Silva, F. D.; Oliveira Junior, V. X.; Lu, T. K.; de la Fuente-Nunez, C. Structure-Function-Guided Exploration of the Antimicrobial Peptide Polybia-CP Identifies Activity Determinants and Generates Synthetic Therapeutic Candidates. *Communications Biology* **2018**, *1* (1), 221.
- (65) Pedron, C. N.; Torres, M. D. T.; Lima, J. A. D. S.; Silva, P. I.; Silva, F. D.; Oliveira, V. X. Novel Designed VmCT1 Analogs with Increased Antimicrobial Activity. *Eur. J. Med. Chem.* **2017**, *126*, 456.
- (66) Torres, M. D. T.; Pedron, C. N.; da Silva Lima, J. A.; da Silva, P. I.; da Silva, F. D.; Oliveira, V. X. Antimicrobial Activity of Leucine-Substituted Decoralin Analogs with Lower Hemolytic Activity. *Journal of Peptide Science* **2017**, *23*, 818–823.
- (67) Torres, M. D. T.; Pedron, C. N.; Araújo, I.; Silva, P. I.; Silva, F. D.; Oliveira, V. X. Decoralin Analogs with Increased Resistance to Degradation and Lower Hemolytic Activity. *ChemistrySelect* **2017**, *2* (1), 18–23.
- (68) Grishin, D. v.; Zhdanov, D. D.; Pokrovskaya, M. v.; Sokolov, N. N. D-Amino Acids in Nature, Agriculture and Biomedicine. *All Life* **2020**, *13* (1), 11–22.
- (69) Dryden, M. S. Complicated Skin and Soft Tissue Infection. *J. Antimicrob. Chemother.* **2010**, *65*, iii35–iii44.
- (70) Becerra, S. C.; Roy, D. C.; Sanchez, C. J.; Christy, R. J.; Burmeister, D. M. An Optimized Staining Technique for the Detection of Gram Positive and Gram Negative Bacteria within Tissue. *BMC Res. Notes* **2016**, *9* (1), 216 DOI: 10.1186/s13104-016-1902-0.
- (71) Serra, R.; Grande, R.; Butrico, L.; Rossi, A.; Settimio, U. F.; Caroleo, B.; Amato, B.; Gallelli, L.; de Franciscis, S. Chronic Wound Infections: The Role of Pseudomonas Aeruginosa and Staphylococcus Aureus. *Expert Review of Anti-infective Therapy* **2015**, *13* (5), 605–613.
- (72) Gaglione, R.; Smaldone, G.; Cesaro, A.; Rumolo, M.; De Luca, M.; Di Girolamo, R.; Petraccone, L.; Del Vecchio, P.; Oliva, R.; Notomista, E.; Pedone, E.; Arciello, A. Impact of a Single Point Mutation on the Antimicrobial and Fibrillogenic Properties of Cryptides from Human Apolipoprotein B. *Pharmaceuticals* **2021**, *14* (7), 631.
- (73) Powell, M. F.; Stewart, T.; Otvos, L., Jr.; Urge, L.; Gaeta, F. C. A.; Sette, A.; Arrhenius, T.; Thomson, D.; Soda, K.; Colon, S. M. Peptide Stability in Drug Development. II. Effect of Single Amino Acid Substitution and Glycosylation on Peptide Reactivity in Human Serum. *Pharm. Res.* **1993**, *10* (9), 1268–1273.
- (74) Torres, M. D. T.; Pedron, C. N.; Araújo, I.; Silva, P. I.; Silva, F. D.; Oliveira, V. X. Decoralin Analogs with Increased Resistance to Degradation and Lower Hemolytic Activity. *ChemistrySelect* **2017**, *2* (1), 18.
- (75) Gaglione, R.; Cesaro, A.; Dell'Olmo, E.; Di Girolamo, R.; Tartaglione, L.; Pizzo, E.; Arciello, A. Cryptides Identified in Human Apolipoprotein B as New Weapons to Fight Antibiotic Resistance in Cystic Fibrosis Disease. *International Journal of Molecular Sciences* **2020**, *21* (6), 2049.
- (76) Dell'Olmo, E.; Gaglione, R.; Sabbah, M.; Schibeci, M.; Cesaro, A.; Di Girolamo, R.; Porta, R.; Arciello, A. Host Defense Peptides Identified in Human Apolipoprotein B as Novel Food Biopreservatives and Active Coating Components. *Food Microbiology* **2021**, *99*, 103804.
- (77) Gaglione, R.; Cesaro, A.; Dell'Olmo, E.; Di Girolamo, R.; Tartaglione, L.; Pizzo, E.; Arciello, A. Cryptides Identified in Human Apolipoprotein b as New Weapons to Fight Antibiotic Resistance in Cystic Fibrosis Disease. *Int. J. Mol. Sci.* **2020**, *21* (6), 2049.
- (78) Gaglione, R.; Pirone, L.; Farina, B.; Fusco, S.; Smaldone, G.; Aulitto, M.; Dell'Olmo, E.; Roscetto, E.; Del Gatto, A.; Fattorusso, R.; Notomista, E.; Zaccaro, L.; Arciello, A.; Pedone, E.; Contursi, P. Insights into the Anticancer Properties of the First Antimicrobial Peptide from Archaea. *Biochimica et Biophysica Acta (BBA) - General Subjects* **2017**, *1861* (9), 2155–2164.



JACS Au
AN OPEN ACCESS JOURNAL OF THE AMERICAN CHEMICAL SOCIETY

Editor-in-Chief
Prof. Christopher W. Jones
Georgia Institute of Technology, USA

Open for Submissions 

pubs.acs.org/jacsau  ACS Publications
Most Trusted. Most Cited. Most Read.